

An initial volcanic hazard assessment of the Vestmannaeyjar Volcanic System: Impacts of lava flow and tephra deposit on Heimaey

Melissa Anne Pfeffer, Sara Barsotti, Esther Hlíðar Jensen, Emmanuel Pierre Pagneux, Bogi Brynjar Björnsson, Guðrún Jóhannesdóttir, Ármann Höskuldsson, Laura Sandri, Jacopo Selva, Simone Tarquini, Mattia de´ Michieli Vitturi, Ingibjörg Jónsdóttir, Davið Egilson, Marine Giroud, Sigrún Karlsdóttir, Bergrún Óladóttir, Matthew J. Roberts, Kristín Vogfjörð, Jórunn Harðardóttir

An initial volcanic hazard assessment of the Vestmannaeyjar Volcanic System: Impacts of lava flow and tephra deposit on Heimaey

Melissa Anne Pfeffer¹, Sara Barsotti¹, Esther Hlíðar Jensen¹, Emmanuel Pierre Pagneux^{1,7}, Bogi Brynjar Björnsson¹, Guðrún Jóhannesdóttir², Ármann Höskuldsson³, Laura Sandri⁴, Jacopo Selva⁴, Simone Tarquini⁵, Mattia de Michieli Vitturi⁵, Ingibjörg Jónsdóttir⁶, Davið Egilson¹, Marine Giroud⁸, Sigrún Karlsdóttir¹, Bergrún Óladóttir^{1,3}, Matthew J. Roberts¹, Kristín S. Vogfjörð¹, Jórunn Harðardóttir¹

¹ Veðurstofa Íslands

² Almannavarnadeild Ríkislögreglustjóra

³ Jarðvísindastofnun Háskólans

⁴ Istituto Nazionale di Geofisica e Vulcanologia (INGV), Bologna

⁵ Istituto Nazionale di Geofisica e Vulcanologia (INGV), Pisa

⁶ Jarðvísindadeild Háskóla Íslands

⁷ Agricultural University of Iceland

⁸ Consultant

Skýrsla nr. VÍ 2020-011	Dags. Desember 2020	ISSN 1670-8261	Opin <input checked="" type="checkbox"/> Lokuð <input type="checkbox"/> Skilmálar:
Heiti skýrslu / Aðal- og undirtitill: An initial volcanic hazard assessment of the Vestmannaeyjar Volcanic System: Impacts of lava flow and tephra deposit on Heimaey			Upplag: 20 Fjöldi síðna: 73
			Framkvæmdastjóri sviðs: Jórunn Harðardóttir
Höfundar: Melissa Anne Pfeffer, Sara Barsotti, Esther Hlíðar Jensen, Emmanuel Pierre Pagneux, Bogi Brynjar Björnsson, Guðrún Jóhannesdóttir, Ármann Höskuldsson, Laura Sandri, Jacopo Selva, Simone Tarquini, Mattia de Michieli Vitturi, Ingibjörg Jónsdóttir, Davíð Egilson, Marine Giroud, Sigrún Karlsdóttir, Bergrún Óladóttir, Matthew J. Roberts, Kristín Vogfjörð, Jórunn Harðardóttir			Verkefnisstjóri: Melissa Anne Pfeffer
			Verknúmer: 3721-0-0004
Gerð skýrslu/verkstig: Uppfært í desember 2021			Málsnúmer: 2018-0172
Unnið fyrir: Ofanflóðasjóð, ICAO			
Samvinnuaðilar: Almannavarnadeild ríkislögreglustjóra, Háskóli Íslands, INGV, Verkís			
Útdráttur: This report is an initial assessment of phenomena and events from the Vestmannaeyjar volcanic system that may potentially be harmful to people and cause damages to infrastructure on Heimaey. Lava flow emplacement and tephra fallout have been modeled from potential future eruption scenarios for estimating possible damages to critical infrastructure. This report can be used for long-term planning between eruptions. Model results show that there is only a 3–8% likelihood that the next eruption from the Vestmannaeyjar volcanic system will open on Heimaey itself. The most densely populated parts of Heimaey in the north and around the harbor are the most vulnerable areas to lava flows originating on the island. Half of the residential roofs are vulnerable to collapse from tephra loading within six days of a moderate eruption if the eruption emerges close to Heimaey, if the winds promote transport over the island, if it is raining or snowing, and if no mitigation actions are taken: otherwise the tephra is unlikely to collapse many homes. We recommend that more foundational work on the ages of identifiable vents, gases and flammable ballistics be done so that the model of future vent location probability can be improved, temporal likelihood of future eruptions can be calculated, and these additional hazards can be assessed.			
Lykilorð: Volcanic hazard assessment, Vestmannaeyjar, lava flow, tephra deposit, Heimaey			Undirskrift framkvæmdastjóra sviðs:
			Undirskrift verkefnisstjóra:
			Yfirfarið af: SG

Contents

ABSTRACT	8
1 INTRODUCTION.....	9
1.1 Long-term volcanic hazard assessment.....	9
1.2 Study strategy.....	10
1.3 Framework of the project.....	11
1.4 Definitions of italicized terms used within this report	13
2 GEOLOGY, PAST AND CURRENT ACTIVITY, AND GEOGRAPHY.....	14
2.1 Geology.....	14
2.2 Previous eruptions.....	15
2.3 Lava flows from previous eruptions	17
2.4 Tephra deposits from previous eruptions.....	19
2.5 Current level of activity	19
3 HAZARDS, UNDERLYING METHODS AND DEFINED ERUPTION SCENARIOS	20
3.1 Event tree	20
3.2 Lava inundation model.....	22
3.3 Potential lava inundation from hypothetical eruptions	24
3.4 Tephra mass loading	29
3.5 Tephra dispersal and deposition model.....	29
3.6 Potential tephra deposition from hypothetical eruptions	34
3.7 Modeled locations of potential future eruptions	37
4 EXPOSURE	41
4.1 Critical infrastructure	41
4.2 People.....	41
5 IMPACTS.....	42
5.1 Lava inundation.....	42
5.2 Tephra fall.....	42
5.2.1 Roads and airport runways	43
5.2.2 Mass loading on buildings	43
5.3 Direct economic costs	45
6 MITIGATION AND PREPAREDNESS	47
6.1 Warning and forecasting	47
6.1.1 Pre-eruption monitoring.....	47
6.1.2 Communication of risk	49
6.2 Risk acceptance.....	50
6.3 Comprehensive risk assessment.....	50
6.4 Knowledge building in society.....	50

6.5	Evacuation response plans.....	51
6.6	Mitigation.....	52
7	CONCLUSIONS AND RECOMMENDATIONS.....	53
7.1	Conclusions.....	53
7.2	Recommendations.....	54
8	ACKNOWLEDGMENTS.....	55
	REFERENCES.....	56
	APPENDICES.....	60
A.	DEM, bathymetry, and topography.....	60
B.	Input parameters used to run the mrlavaloba simulations.....	61
C.	Grain size distribution from heimaey 1973 eruption.....	64
D.	Age of vents relative to best fit line.....	65
E.	Weight-bearing capacity of homes in heimaey.....	67
F.	How to contextualize the probabilities given in this report.....	69

Figures

Figure 1:	Map of Iceland featuring the main central volcanoes, fissure swarms, main volcanic belts and populated areas that could be particularly vulnerable to effusive eruption products ..	11
Figure 2:	Bathymetry and topography of the Vestmannaeyjar volcanic system	15
Figure 3:	Map of Heimaey	16
Figure 4:	Isopach lines of the cumulative thickness of tephra deposits during the 1973 Eldfell eruption	19
Figure 5:	Event tree for the Vestmannaeyjar volcanic system.....	21
Figure 6:	Map of Heimaey showing the regular, gridded locations where modelled lava flows originated	25
Figure 7:	Modeled extent and thickness of lava from Small, Moderate, and Large eruptions originating from a single vent location in downtown	26
Figure 8:	The likelihood that locations on Heimaey will be inundated by lava given a Small, Moderate, or Large eruption anywhere on the island	27
Figure 9:	Areas where eruptions could originate whose lava could impact areas of interest ..	28
Figure 10:	Daily maximum plume heights observed during the 1973 eruption	31
Figure 11:	Total grain size distribution of lapilli and ash measured during the 1973 Eldfell eruption	32
Figure 12:	Moderate sized eruptions with six days duration from a vent at Eldfell	34
Figure 13:	Vertical profile of the wind direction and wind speed for the worst case and best case simulations	35

Figure 14: The probability that tephra (<64 mm) released from a six-day long Moderate eruption at Eldfell and Surtsey would form a 3 cm thick deposit on Heimaey	36
Figure 15: Frequency of wind direction and wind speed.....	37
Figure 16: Probability of location of future vent opening based on the best fit line of the identified previous vents.....	38
Figure 17: Probability of location of future vent opening based on the locations of identified previous vents using a Gaussian kernel-smoothed function model.....	39
Figure 18: Monthly foreign visitors to Heimaey in 2016	42
Figure 19: The probability that tephra released from a six-day-long Moderate eruption at Eldfell and Surtsey would form a 0.1–0.5 cm thick deposit on Heimaey	44
Figure 20: Exceedance probabilities for accumulation of tephra from a vent at Eldfell	45
Figure 21: Direct economic cost of infrastructure destruction for the different eruption scenarios	48
Figure 22: Spatial distribution of identified vents and the best fit line of their locations.....	65
Figure 23: Distance from the best fit line of identified vents by age.....	66
Figure 24: Simulated mass loading (tephra + precipitation) for 23–29 January 1973 during the Eldfell eruption	68

Tables

Table 1: Properties of selected Vestmannaeyjar lava flows.	18
Table 2: Characterization of the three different eruption size scenarios	24
Table 3: Terminology used in the report for pyroclastic material and its size	29
Table 4: Eruption source parameters measured in the 1973 Eldfell eruption.....	33
Table 5: The cumulative mass and average size distribution of tephra samples	64
Table 6: Mass load capacity of Vestmannaeyjar residences.....	67
Table 7: Potential economic impact in Heimaey using an acceptable risk threshold of 5% for tephra deposits and lava inundation.....	70
Table 8: Potential economic impact in Heimaey using an acceptable risk threshold of 25% for tephra deposits and lava inundation.....	72

Abstract

This work is the first step of a comprehensive long-term volcanic hazard assessment of the Vestmannaeyjar volcanic system focusing on critical infrastructure on Heimaey and is suitable for long-term planning during the quiescent time between eruptions. It can be further developed after more geologic mapping and dating of deposits has been made to include more knowledge of the eruptive history and the magmatic system and be refined after acceptable volcanic risk in Iceland has been defined. Probabilistic modeling of lava flows and tephra fall from potential future eruption scenarios is used to analyze how different eruption conditions produce hazards of different sizes from various locations. The impacts of the hazards on the community are quantified by considering their potential to destroy critical infrastructure and the resulting potential economic damage in the absence of mitigation actions. Eruption frequency for the Vestmannaeyjar volcanic system is low relative to the frequently active volcanoes of the Eastern Volcanic Zone. In the case of an eruption within the whole system there is only a 3–8% likelihood that a vent will open on Heimaey. In other words, there is a 92–97% likelihood that the next eruption within the volcanic system will not be on Heimaey. The most densely populated parts of Heimaey in the north and around the harbor are the most vulnerable to Moderate and Large lava flows originating on the island. Almost all infrastructure on the island is vulnerable to lava inundation from a Large eruption originating anywhere on the island. Half of the Heimaey residence roofs are at risk of collapsing due to tephra load within six days of some Moderate sized eruptions only if an eruption occurs on or close to Heimaey; if the winds promote transport over the island; and if the tephra is wet (as precipitation adds to the mass). Mitigation actions have proved to be extremely beneficial and the experiences from the 1973 eruption should be relied on to help with future actions. Pre-eruption mitigation can occur in a variety of ways including Civil Protection contingency planning, building up specialist knowledge and within vulnerable communities and via land-use planning.

1 Introduction

This work is an initial long-term *volcanic hazard*¹ assessment of the Vestmannaeyjar volcanic system focusing on *critical infrastructure* on Heimaey, the only inhabited island of the Vestmannaeyjar archipelago, Iceland. Hazard assessment, as an estimation of phenomena and events that may potentially be harmful to people and cause damages, is an essential element of *disaster risk assessment* (Bobrowsky, 2013). This study has investigated and quantified the economic impact on Heimaey in the event of an eruption in the archipelago. This has been done by using numerical models to simulate lava flow emplacement and tephra fallout for estimating the potential damages to critical infrastructure.

Critical infrastructure on Heimaey includes residences, community-use facilities, roads, power and water supplies, businesses, the harbor, and the airport: assets that are essential for the safety, health, security, and economy of the community. The economic value of critical infrastructure potentially harmed by lava and mass loading from tephra during future eruptive activity of the Vestmannaeyjar volcanic system was assessed in this report using November 2017 values.

1.1 Long-term volcanic hazard assessment

The analysis presented here is intended to be an initial step of a comprehensive long-term assessment of volcanic hazards that can be developed as we gain more thorough understanding of the geological background of the volcanic system. Long-term volcanic hazard assessments should include the temporal likelihood of eruption occurrence, but we did not attempt to do this in this work, due to limited foundational knowledge. This should be added in future studies. The results of the work can be applied even though it lacks an absolute eruption likelihood assessment. This preliminary work can be useful in the quiescent time between eruptions for use in long-term land-use planning, for cost-benefit analysis of potential mitigation actions, and it provides a range of possibilities for response planning. The assessment is based on what is currently known about the volcanic system and utilizes hypothetical eruption parameters and detailed numerical models that require a long time to run.

During the build-up to an eruption, a short-term assessment will be needed, and a different methodology would be preferred. In such circumstances, real-time monitoring data would gain importance and the most-likely potential scenarios might be constrained by these observations. Moreover, the simulation results and maps might be updated to reflect new sources of information and the usage of the maps would go more towards assisting the response planning.

During an eruption, the methodology would change again, and the hazard assessment would be revisited continually based on the real-time monitoring. The scenarios would be defined based on what is occurring (potential future changes in the activity would also be considered), and the models used would have simpler physics so that they could be run in as close to real time as possible (operational models). Furthermore, the products provided would include short-term forecasts, which would be used to anticipate short-term future changes in the eruptive behavior and to focus on assisting evacuation and mitigation activities.

¹ All italicized terms are defined in Section 1.4

An exclusive emphasis on long-term hazard assessment, focused solely on infrastructure, is insufficient when a volcanic crisis is ongoing as our primary goal then is to minimize fatalities and harm to people. The shorter-term and human aspects have been addressed in this report by drawing on information that has already been provided by other agencies, including tourist and permanent population data (Section 4.2), a description of the early warning system (Section 6.1) and summaries of related previous work (Sections 6.4 and 6.5).

1.2 Study strategy

Within this work, eruption scenarios were defined based on past activity as observed or measured or recorded in the geologic record (Sections 2.2, 2.3, 2.4 and 3.1). Lava flow simulations were performed to capture a range of possible eruption strengths and eruption vent locations on Heimaey. Tephra dispersion and deposition simulations were performed to capture a variety of weather conditions and two different vent locations within the Vestmannaeyjar system. The simulations were performed based on defined scenarios (Sections 3.3 and 3.6).

Individual simulations produce so-called deterministic solutions, which are then integrated to produce the probabilistic hazard maps that are the primary results of this hazard report. The probabilistic maps produced by integrating the deterministic simulations show how probable, or likely, a hazard is at a given location. The interplay between deterministic and probabilistic approaches to forecasting volcanic activity is discussed in Rouwet et al. (2017). These maps show how different eruption conditions can produce differently located and sized hazards, and how these differences are reflected in the economic damage that could be caused by hypothetical future eruptions. The locations of homes and other critical infrastructure (Section 4.1) were used in relation to the spatial likelihood of the hazards to analyze potential economic harm from damage to or destruction of the infrastructure (Section 5.3). We made a detailed study of the weight-bearing capacity of homes on Heimaey (0). We have provided recommendations for long-term planning on the island (Section 7.2) and have provided a plan for dissemination of the report's results (Section 6.4).

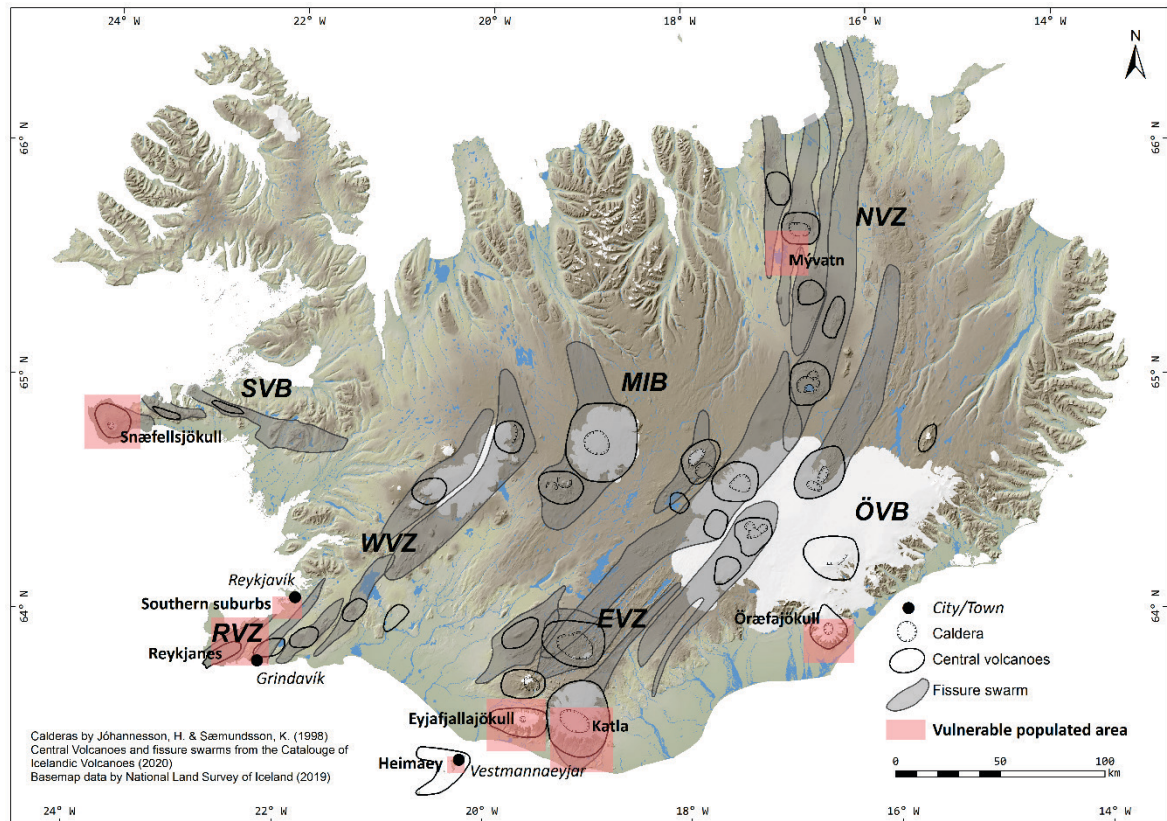


Figure 1: Map of Iceland featuring the main central volcanoes, fissure swarms, main volcanic belts and populated areas that could be particularly vulnerable to effusive eruption products (red) Mid Iceland Belt (MIB), Northern Volcanic Zone (NVZ), Snæfellsnes and Örfæfjökull Volcanic Belts (SVB and ÖVB) (based on Jóhannesson & Sæmundsson, 1998; Thordarson & Larsen, 2007). The Vestmannaeyjar volcanic system is displayed as having a horseshoe-shaped central volcano as in Jóhannesson and Sæmundsson (1998). This shape reflects the pattern of submarine land seen in the bathymetry data. The central volcano of the Vestmannaeyjar system is considered embryonic and resultingly ill-defined. The horseshoe shape depicted here is not reflected in the distribution of submarine vents identified later in this report.

1.3 Framework of the project

The 1973 Eldfell eruption crisis and citizen response on Heimaey provides a classic example of the risks to, and *mitigation* actions that can be taken by, communities close to volcanoes. The fissure was located only 200 m east of the town, whose infrastructure was significantly harmed by the eruption. Over 5,000 inhabitants of Heimaey were successfully evacuated during the first hours of the eruption and only one person died due to *hazards* produced during the event. A summary of the deaths and economic cost of natural hazards in Iceland from the last two centuries found that the Eldfell eruption was by far the most expensive, costing about 320 million Euros in April 2017 values, or 60‰ of Iceland’s GDP (Jóhannesson, 2017).

When the source of a hazard (eruption vent) is close to a vulnerable community (proximal), the community’s *exposure* is quite different than where the source of the hazard is distal to the

community. Proximal volcanic hazards on Heimaey due to an eruption within the Vestmannaeyjar volcanic system include lava flows, tephra fall, toxic gases, lightning, and ballistics. Within this report, we focus on the hazards from lava flow inundation and mass loading from tephra fall, due to more complete records of lava and tephra hazards from previous eruptions. There are additional distal hazards on Heimaey due to eruptions at other Icelandic volcanoes, which could include tephra fall and tsunamis. These distal hazards are not examined in this report due to its focus on proximal hazards.

This report is one component of GOSVÁ, Iceland's national volcanic hazard assessment program funded by the National Avalanche and Landslide Fund. Led by the Icelandic Meteorological Office (IMO), the steering committee of GOSVÁ includes representatives from IMO, the Institute of Earth Sciences (IES, University of Iceland), the Department of Civil Protection and Emergency Management of the National Commissioner of the Icelandic Police (NCIP-DCPEM), the Soil Conservation Service of Iceland (SCSI), and the Icelandic Road and Coastal Administration. The goal of GOSVÁ is to minimize loss of life, limit/prevent an increase of risk in the future and minimize economic disruption to and damages in society.

Several projects have been completed so far in the GOSVÁ program, including an appraisal of the current knowledge of the past eruptive activity and potential hazards of Icelandic volcanoes, available as the on-line Catalogue of Icelandic Volcanoes at <http://icelandicvolcanoes.is> and a preliminary hazard and risk assessment focusing on glacial outbursts caused by eruptions of Katla and Örfajökull volcanoes (Pagneux et al., 2015). This report fulfils part of the project **Initial hazard assessment of volcanic eruptions that may cause extensive damage to infrastructure**. The project was funded by the National Avalanche and Landslide Fund and the International Civil Aviation Organization (ICAO). Iceland is signatory to the Sendai Framework for Disaster Risk Reduction (2015–2030). The framework adheres to the International Strategy for Disaster Reduction system supported by the United Nations Office for Disaster Risk Reduction (UNDRR, formerly known as UNISDR), which is used as a guideline for all the risk and hazard assessment projects that have been made by the IMO on behalf of the Icelandic government to strengthen the *resilience* of Iceland to disasters.

This English report is a technical supplement to the Icelandic report *Forgreining á hættu vegna goss á eldstöðvakerfi Vestmannaeyja. Frummat á áhrifum hraunrennslis og öskufalls í Heimaey* (Pfeffer et al., 2021). This is a preliminary report, which serves as an initial step towards ever-improving future volcanic risk and hazard assessments in Vestmannaeyjar and other vulnerable regions of Iceland. The needs of vulnerable communities, available foundational knowledge, and available tools all change over time. There are continual improvements and advancements in the fields of geology and risk and hazard assessments. Future effusive eruptions are likely to affect populated areas in Iceland. Heimaey, as well as the areas including the southern suburbs of Reykjavík (Kópavogur, Garðabær, and Hafnarfjörður); the Reykjanes peninsula including Grindavík; the Mývatn region; and the lowlands around Snæfellsjökull; Eyjafjallajökull, Mýrdalsjökull (Katla), and Örfajökull are particularly *vulnerable* (Figure 1; Gudmundsson et al., 2008). We hope that this report, and those that will be prepared in the future, will be beneficial for vulnerable communities.

1.4 Definitions of italicized terms used within this report

Below are the definitions for italicized terms used within this report as provided by UNDRR.

Critical infrastructure: The physical structures, facilities, networks and other assets which provide services that are essential to the social and economic functioning of a community or society.

Disaster risk: The potential loss of life, injury, or destroyed or damaged assets which could occur to a system, society or a community in a specific period of time, determined probabilistically as a function of hazard, exposure, vulnerability and capacity.

Disaster risk assessment: A qualitative or quantitative approach to determine the nature and extent of disaster risk by analyzing potential hazards and evaluating existing conditions of exposure and vulnerability that together could harm people, property, services, livelihoods and the environment on which they depend.

Early warning system: An integrated system of hazard monitoring, forecasting and prediction, disaster risk assessment, communication and preparedness activities systems and processes that enables individuals, communities, governments, businesses and others to take timely action to reduce disaster risks in advance of hazardous events.

Exposure: The situation of people, infrastructure, housing, production capacities and other tangible human assets located in hazard-prone areas.

Hazard: A process, phenomenon or human activity that may cause loss of life, injury or other health impacts, property damage, social and economic disruption or environmental degradation.

Mitigation: The lessening or minimizing of the adverse impacts of a hazardous event.

Resilience: The ability of a system, community or society exposed to hazards to resist, absorb, accommodate, adapt to, transform and recover from the effects of a hazard in a timely and efficient manner, including through the preservation and restoration of its essential basic structures and functions through risk management.

Volcanic hazards: Volcanic activity and emissions are examples of **Geological or geophysical hazards** (the term defined by the UNISDR) that originate from internal earth processes.

Vulnerability: The conditions determined by physical, social, economic and environmental factors or processes which increase the susceptibility of an individual, a community, assets or systems to the impacts of hazards.

2 Geology, Past and Current Activity, and Geography

2.1 Geology

Elevated volcanic activity in Iceland is caused by the superposition of the North Atlantic ridge system on the Icelandic mantle plume (e.g., Sæmundsson, 1974; Vink, 1984; White et al., 1995; Wolfe et al, 1997). The main volcanism is centered on several zones extending from Reykjanes through Western and Northern Volcanic Zones (RVZ, WVZ, and NVZ), which are connected by the Mid-Iceland Belt (MIB). In addition, the Eastern Volcanic Zone (EVZ) stretches to the southeast from the assumed center of the Icelandic mantle plume and is by far the most active volcanic belt in Iceland. Other active volcanic areas include the Snæfellsnes and Örfajökull belts (SVB and ÖVB) (Figure 1) (see e.g. Thordarson & Larsen, 2007). The EVZ is a propagating rift zone (Meyer et al., 1985; Mattson & Höskuldsson, 2003) characterized by rifting features (open fractures and faults) in the northern part but no indication of active rifting in the southern part where Vestmannaeyjar is located.

The Vestmannaeyjar volcanic system is one of nine active volcanic systems of the EVZ (Jóhannesson & Sæmundsson, 1998). The system does not have a well-developed central volcano nor a fissure swarm (see e.g. Jakobsson, 1968; 1979; Mattson & Höskuldsson, 2003; Höskuldsson, 2015). It is made of clusters of short eruptive fissures that are seen today as a NE-SW trending 32 km long archipelago formed of islands and skerries which are the remains of volcanic craters and islands (Jakobsson, 1979; Thordarson & Larsen, 2007). Due to the submerged nature of much of the system, it is considerably less well studied than on-land systems. The archipelago has formed over the last 70–120 thousand years and the currently visible features were produced during volcanic eruptions during the last 14–20 ka (Höskuldsson et al., 2013). There are currently between 15–18 islands and skerries and 45–75 submarine peaks (differing based on definition used while counting). In this work, we have identified 47 vents or places of past eruptions based on landscape morphology (Figure 2, 0). Additional vents may have been covered by younger deposits, eroded, lie outside of the mapped area, and/or have been incorrectly identified as not a vent. Volcanic production has been greatest around Heimaey, Surtsey and Geirfuglasker where the islands and mounds are most prominent. The dating and chronology of submerged mounds and several islands is inadequately known.

Volcanism in Vestmannaeyjar is understood to be low, in terms of both eruption frequency and magma production as compared with the other volcanic systems on the EVZ such as Grímsvötn and Bárðarbunga, the most active systems in Iceland. The current behavior of the Vestmannaeyjar volcanic system includes long quiet periods with no activity at about millennial time scales. The short interval over which different tephra layers have been deposited, such as in Northern Heimaey, are indicative of episodic behavior (Jakobsson, 1979). Each eruption can last from months to years, and clusters of eruptions can last from decades to centuries (Mattson & Höskuldsson, 2003). Past and potential future eruptions from Vestmannaeyjar are categorized as small (eruptive products $< 0.1 \text{ km}^3$), moderate ($0.1\text{--}0.5 \text{ km}^3$), and large ($> 0.5 \text{ km}^3$) in the CIV. The largest known eruption was the 1963–1967 Surtsey eruption.

The system produces magma from alkali basalt to mugearite which is consistent with the young ($< 100 \text{ ka}$) age of the system (Jakobsson, 1979). The islands of Vestmannaeyjar are mostly made of tuff and pillow lava with subaerial lava on Heimaey and Surtsey. Heimaey is composed primarily of materials from previous eruptions (as well as some non-consolidated sediments) demonstrating the vulnerability of the entire island during future eruptions (Figure 3).

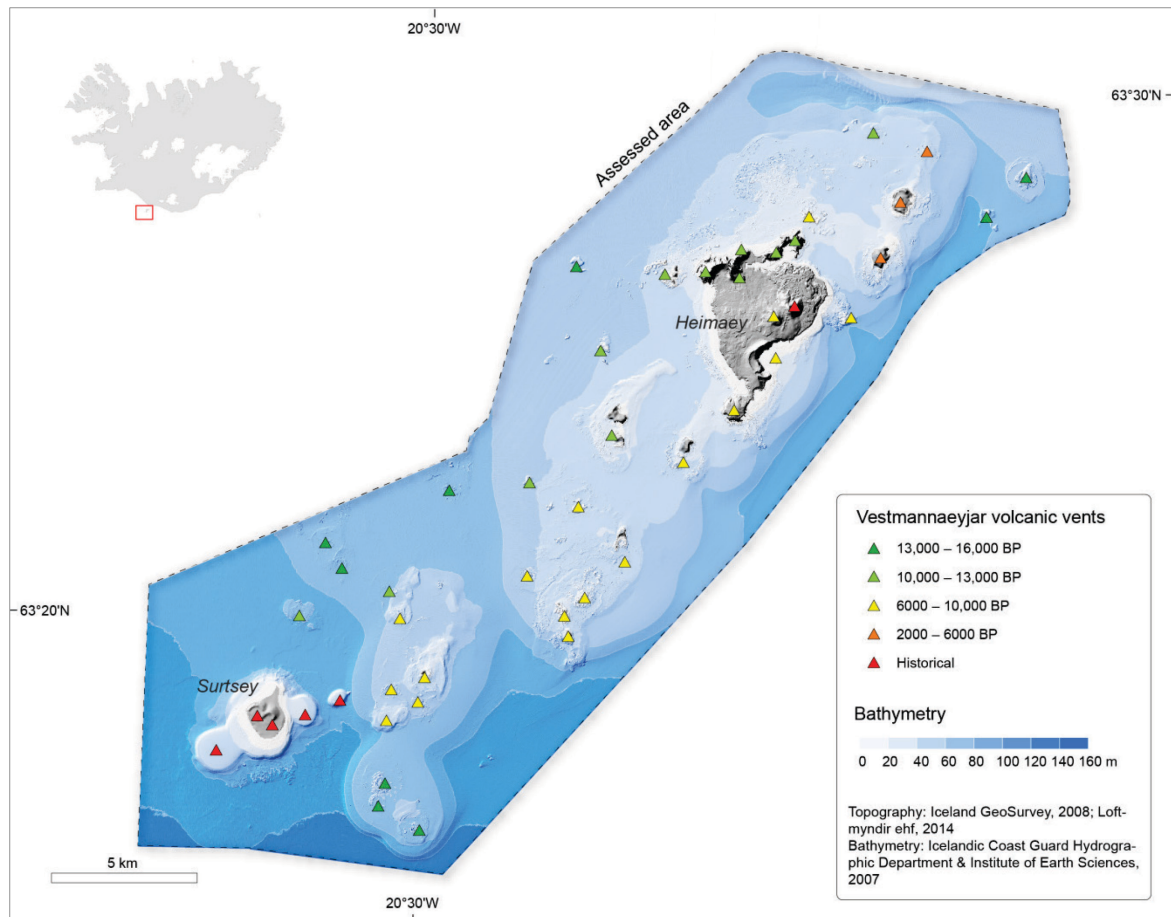


Figure 2: Bathymetry and topography of the Vestmannaeyjar volcanic system (Icelandic Coast Guard Hydrographic Department & University of Iceland Institute of Earth Sciences, 2007, Iceland GeoSurvey, 2008). Identified vents are indicated by triangles with their ages indicated by color.

2.2 Previous eruptions

The most recent eruptive episode of the Vestmannaeyjar system (1963–1973) included the Surtsey (1963–1967) and Eldfell (1973) eruptions. Surtsey falls in the large sized eruption category and Eldfell in moderate. The Surtsey eruption and the following evolution of the island and the life on it was observed and researched in detail by the Surtsey Research Society (www.surtsey.is). The Surtsey eruption began as a submarine eruption until the newly constructed cone breached the water surface, ending as a subaerial eruption. It lasted 3.5 years and included several distinct phases of eruptive activity.

The Eldfell eruption on Heimaey, with less sea water interaction than Surtsey, lasted about five months, and is an example of a predominantly subaerial eruption producing predominantly lava and some tephra. Óskar J. Sigurðsson, weather observer in Stórhöfði, Heimaey, recorded his observations of the eruption in his diary of the 1973 Heimaey eruption (Sigurðsson, 1973).

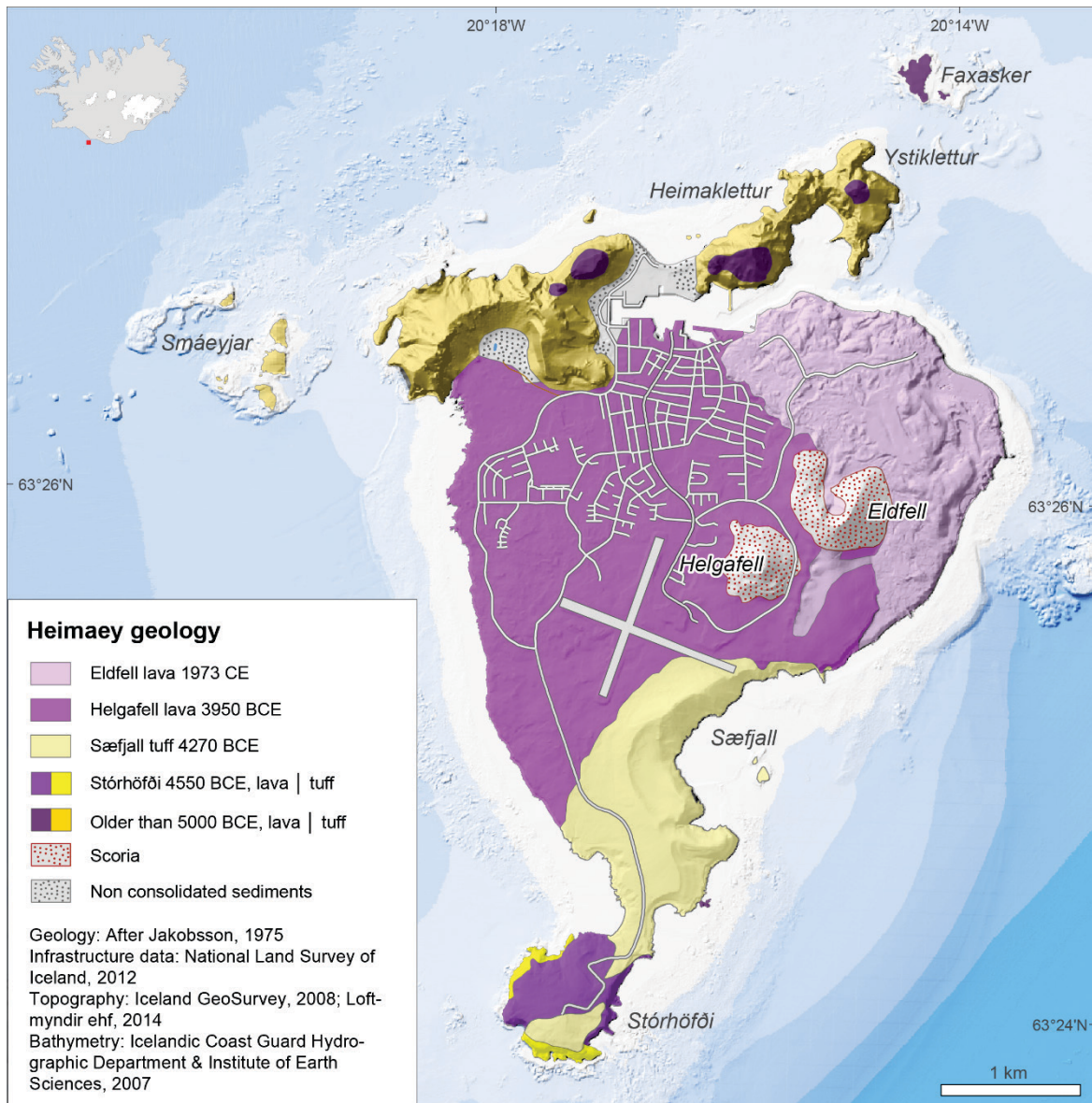


Figure 3: Map of Heimaey. Lavas are shown in purple and tephra deposits in yellow. Older features are indicated by an increase in color saturation. Geology, infrastructure, topography, and bathymetry data from Iceland GeoSurvey, 2008; Icelandic Coast Guard Hydrographic Department & University of Iceland Institute of Earth Sciences, 2007; Jakobsson, 1975; Loftmyndir ehf, 2014; National Land Survey of Iceland, 2012.

Eruptions may also have occurred in 1896 south of Hellisey (Þórarinnsson, 1965), possibly close to Geirfluglasker and in 1637 south-west of Heimaey (Jóhannesson, H., 1983). Other eruptions have been dated using radioactive disequilibrium between isotopes including Helgafell (5,900 years BP; $^{226}\text{Ra}/^{230}\text{Th}$; Sigmarsson, 1996), Sæfjall (sometimes called Sæfell; 6,220 years BP; ^{14}C ; Kjartansson, 1966) and Stórhöfði (at least one century older than Sæfjall; ^{14}C method measured on peat; Kjartansson, 1966). Bjarnaey and Elliðaey are also close in age to Sæfjall and Stórhöfði (Jakobsson, 1979) indicating there was a major volcanic episode between 5,000 – 6,000 years BP. Álsey, Brandur, Surðurey, and Hellisey may be about 8000 years BP based on tephrochronology (Jakobsson, 1979). The Norðurklettar formation (including Blátindur, Dalbjallshryggur, Há, Klif, Heimaklettur, Miðklettur and Ystiklettur) are the oldest deposits on Heimaey, but their age is disputed from ~40,000 years BP (Sigurðsson & Jakobsson, 2009) to ~10,000 years BP (Mattsson & Höskuldsson, 2003). In this report, we have mapped the Norðurklettar formation as being in the 10,000–13,000 years BP age bin (Figure 2, Table 1).

2.3 Lava flows from previous eruptions

Future risk from lava flows can be assessed based on previous lava flow inundation within a specific area, based on the locations and frequency of previous eruptions. The currently visible lava flows of Heimaey are shown in purple colors in Figure 3. In addition to looking at past products, it is also possible to assess future risk by estimating the flow of lava from defined potential future eruptions, based on a range of plausible eruption parameters, which in turn are based on physical properties measured in past eruptions (Table 1).

Table 1: Properties of selected Vestmannaeyjar lava flows.

Eruption	Date	Duration [month]	Lava Volume [km ³]	Lava Volume DRE ² [km ³]	Thickness [m]	Long- axis Length [km]	Flow rate [km ³ / month] ³	Reference
Eldfell	23/01/73–28/06/73	5.1	0.27	0.24	9–100	3.7	0.04	A, B, C, D, E
Surtsey effusive phase 1 ⁴	04/04/64–17/05/65	13.5	?	0.3	max 100	?	>0.02	F, G
Surtsey effusive phase 2 ⁵	19/08/66–05/06/67	9.5	?	0.1	max 70	?	>0.02	F, G
Helgafell	5900 BP	11.5	0.65	0.59	3–50	6.5	<0.06	B, F, H
Klif	12900 BP	?	0.01	0.009	?	?	?	B

References: A: Jakobsson et al., 1973; B: Mattsson & Höskuldsson, 2003; C: Thorarinsson et al., 1973; D: Williams & Moore, 1976; E: This report; F: Mattsson & Höskuldsson, 2005; G: Thordarson, 2000; H: Sigmarsson, 1996

²Lava volume DRE has been calculated using a porosity of 10% as estimated by (Mattsson & Höskuldsson, 2003) for the Helgafell 5900 BP eruption

³The flow rates provided here are eruption averages based on the total volume of lava erupted and the duration of the eruption. Instantaneous measurements of lava flow rates are much higher than these averages, for example during the 1973 Eldfell eruption, lava flow rates of 5.3–99.4 m³/s were measured at different times during the eruption (Williams & Moore, 1976)

⁴ Surtur II lava shield

⁵ Surtur I lava shield

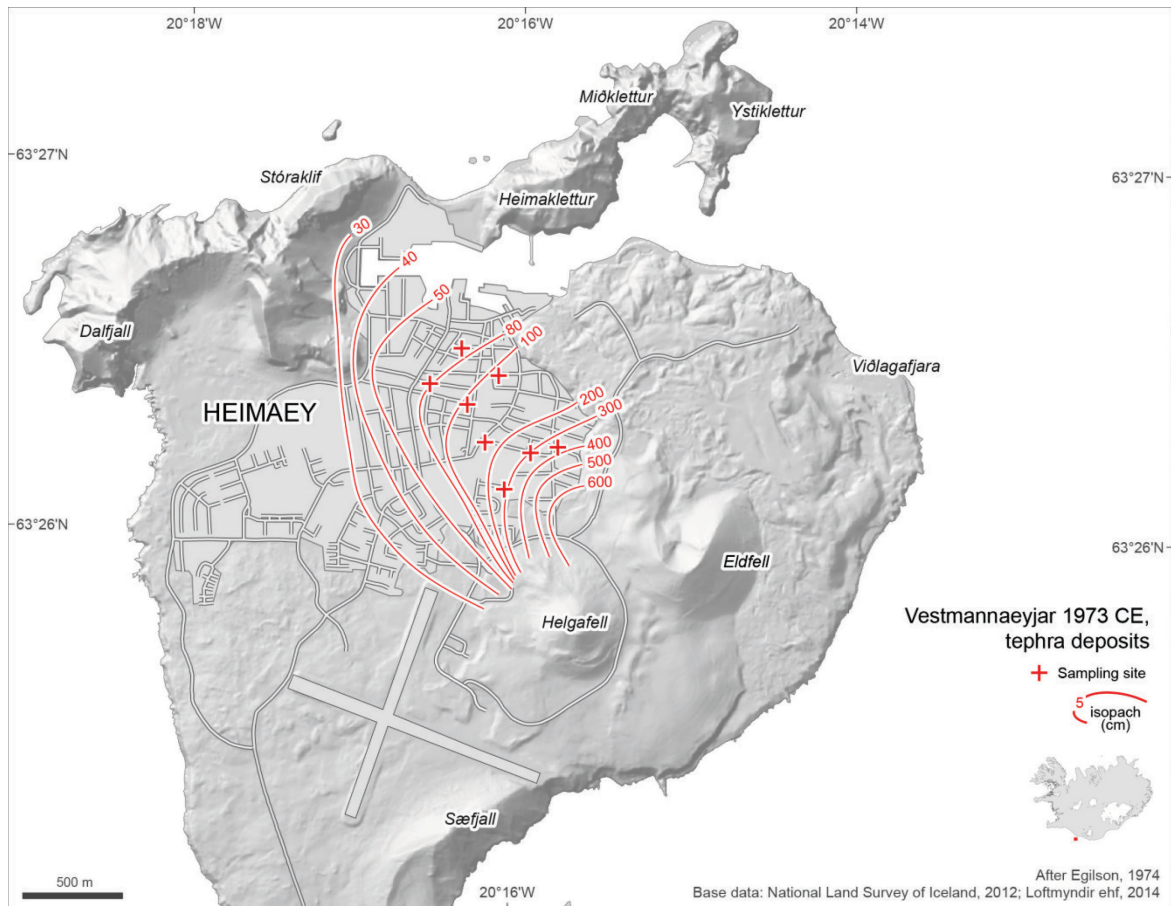


Figure 4: Isopach lines of the cumulative thickness of tephra deposits during the 1973 Eldfell eruption (in cm) as measured during the first month of the eruption (Egilson, 1974).

2.4 Tephra deposits from previous eruptions

The isopach lines of the cumulative thickness of tephra deposits measured at eight sites up to 23/02/1973 from the 1973 Eldfell eruption are shown in Figure 4 from data reported in (Egilson, 1974). The eruption ended on 02/06/1973 but most of the tephra fell until 02/02/1973 so this cumulative thickness is correct for the duration of the entire eruption (Egilson, 1974). The last written report of tephra production was on 26/06/1973 (Sigurðsson, 1973) but this is likely remobilized material that had been previously deposited.

2.5 Current level of activity

As of November 2018, the SIL seismic monitoring network, in operation over the last three decades, shows average background activity levels of around two detectable seismic events at approximately 15 km depth under Heimaey and around four under Surtsey each year. In the last decade, 45 events have been detected between 0.8–3.4 M_l . No significant seismic activity is detected elsewhere in the Vestmannaeyjar system. The continuous deformation network (cGPS) data recorded on Heimaey since 2000 until November 2018 shows no significant deformation signals related to magmatic movements. Periodic analyses of gases released at Eldfell and Surtsey show that the gases contain primarily steam (water) with little magmatic signature.

3 Hazards, underlying methods and defined eruption scenarios

3.1 Event tree

A primary element of long-term volcanic risk assessment is a description of the possible behavior and outcomes of volcanic unrest including size of eruption and types of hazards. One way to frame this description is via an event tree (Newhall & Hoblitt, 2002). An event tree is usually structured in logical steps, taking a form like the branches of a tree that correspond to different possible paths of the volcanic activity. The graphic form of the event tree can be useful for communicating about the uncertainty inherent in eruption forecasts. An event tree includes descriptions of different possible phases of a volcanic event, from a state of unrest extending to the identification of potential hazardous phenomena associated with an eruption. Scenarios displayed in an event tree are based on the knowledge of previous activity, assuming that past activity is the best predictor for future activity but can also include paths based on behavior at analogous volcanoes. Figure 5 shows the event tree for the Vestmannaeyjar volcanic system prepared for this report. The “magnitudes” (total eruptive volume) categories of small, moderate and large and the Associated hazard (volcanic hazards) are the same as used in the Vestmannaeyjar chapter in the CIV (Höskuldsson, 2015). This event tree does not provide information about the relative likelihood of the different paths but conditional probabilities could be added in the future based on expert opinions. The tree could also be extended to include worst case scenarios for hazardous phenomena and/or mitigation actions.

The eruptive hazards that could affect the residents of Heimaey during an eruption in the Vestmannaeyjar system include tephra, gases, lightning, lava, and ballistics (Figure 5, column “Associated hazard”). Within this initial report, we focus on lava inundation and tephra deposition. We utilize numerical models to forecast potential impacts during future eruptions based on past activity. The hazards that can be produced are related to properties of the volcanic eruption itself, such as composition of the erupting magma and the eruption rate, and the interaction of the eruptive materials with the surrounding sea water. If eruptions begin beneath the surface of the sea, the explosivity can be dampened by the pressure from the overlying water column. Tephra production is progressively suppressed as water depth increases from 10–100 m and there is unlikely to be subaerial tephra if the water depth is greater than 100 m (Tonini et al., 2015). Once a vent has built up sufficiently so that the water depth is <10 m, it may behave like a subaerial eruption (Tonini et al., 2015).

A subaerial or sufficiently shallow submarine eruption can produce tephra which can reach a maximum height of ~9–12 km (Sigurgeirsson, 1965; Thorarinnsson et al., 1973). If the vent grows until sea water is no longer contributing to the fragmentation of the erupted material, the production of tephra can slow down and possibly stop as the eruption can evolve into solely lava fountaining and effusive lava flows. More lava will be produced rather than tephra while an eruption of the Vestmannaeyjar system is subaerial. Erupted lava can have further interactions with water, such as by flowing into the sea where toxic gases can be released or interacting with ground water, a lake or a river.

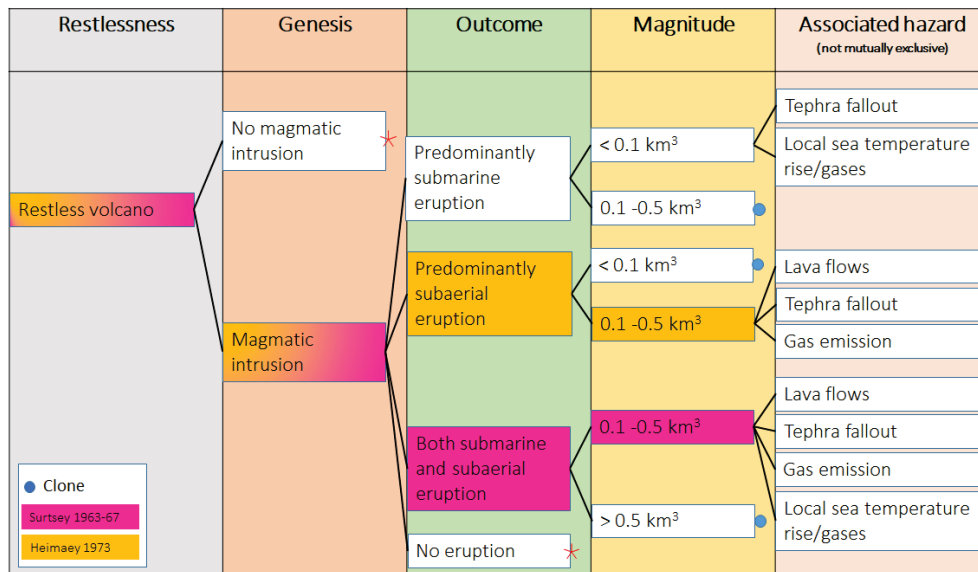


Figure 5: Event tree for the Vestmannaeyjar volcanic system, with the pathways encompassing the behavior exhibited by the 1973 Eldfell and 1963–1967 Surtsey eruptions indicated. The blue dots indicating “clone” show that the phenomena listed previously are replicated for the current junction point. The three magnitude volume ranges correspond to Small, Moderate, and Large eruptions as defined within the CIV (Höskuldsson, 2015).

The lava flow simulations were performed for a range of eruption sizes while the tephra dispersal simulations considered only one eruption size, due to the time necessary to perform the simulations. The lava flow simulations considered three volume scenarios: Small, Moderate, and Large (Table 2) and used the statistical approach of considering a multitude of vent locations on Heimaey. For the tephra simulations, one scenario (a Moderate eruption) at two different locations (Eldfell and Surtsey) with a multitude of meteorological conditions was used to assess the likelihood of impacts resulting from a Moderate eruption originating close to, or far from, Heimaey. The meteorological data is available on grids that are too coarse for the use of more closely spaced vents to be beneficial. We tuned the tephra dispersion and deposition model using data from the Moderate size 1973 Eldfell eruption released from two simulated eruption sites.

Within this work, we have not attempted to model potential pollution impacts of volcanic eruptions on air and water quality in Heimaey. We do not have enough information on the composition and emission rate of gases most likely to be emitted from a Vestmannaeyjar volcanic eruption, and the tephra samples collected during the 1973 Eldfell eruption are too coarse (the particle sizes analyzed are too large) to be used to simulate the potential impacts from the finer, respirable fractions of ash during future events.

Communities very close to an eruption site can be particularly vulnerable to the proximal hazard of air pollution. These impacts can be from gases released from the magma and/or magmatic interactions with water (most notably, SO₂, CO₂, and HF can be harmful to deadly), from aerosol particles formed as the magmatic gases age (most notably, SO₄ aerosol is formed from SO₂ gas), and from tephra particles (the finest ash can be breathed in, and the acidic coatings on tephra particles can acidify and pollute fresh water). One person died due to CO₂ accumulation in a basement during the 1973 Eldfell eruption. During the eruption, rescue

workers needed to be aware of escape routes to higher ground and to ensure proper ventilation when performing mitigation actions inside buildings. As we measure the gases and particles emitted during future Icelandic eruptions with the goal of characterizing these pollutants for use in pollution impact work, we will develop a database that can be used as suitable analogues for other volcanoes. The capacity for considering gas hazards will be built up through a concurrent GOSVÁ project focusing on gas hazards on the Reykjanes Peninsula. We are further working to gain the institutional capacity within Iceland to use a newly developed dense gas dispersion model (Burton et al., 2017) to forecast the dispersion and accumulation in low-lying areas of volcanic CO₂. It is a very high priority to improve our capacity to consider hazards related to volcanic pollution.

3.2 Lava inundation model

MrLavaLoba (de' Michieli Vitturi & Tarquini, 2018), a probabilistic lava settling model, was used to simulate the spread of lava and final lava thicknesses from hypothetical eruptions occurring on Heimaey. This model was initially used for simulating aa and pahoehoe lava flows at Mt Etna and on Hawaii (de' Michieli Vitturi & Tarquini, 2018) and has been successfully applied to the long-lasting Holuhraun lava flow (Tarquini et al., 2018) which formed a large flow field through a variety of emplacement styles (Pedersen et al., 2017). At the time of running the simulations for this report, it was determined that MrLavaLoba was the model most capable of simulating lava flow on relatively flat ground, and of allowing older lava to influence the flow of younger lava during a simulation, because syn-emplacement topographic modifications are accounted for. These features were determined to be important for simulating potential future lava flows on Heimaey. MrLavaLoba treats lava as a series of budding lobes as has been observed in lava flows both on land (e.g., Holuhraun (Pedersen et al., 2017)) and under the sea (e.g., Surtsey (Thordarson, 2000)), indicating that for a first order estimate of lava emplacement, MrLavaLoba is an appropriate model. This model is incapable, however, of providing information on time-evolving changes, such as rate of lava advancement. It is therefore suitable for long-term planning and the consideration of potential economic damages from modeled flows, which are the objective of this report, but not for short-term immediate planning or evacuation during the first stages of an eruption.

The main inputs of the MrLavaLoba code are topography, eruption volume and vent location. Lava does not flow like water and does not strictly follow the maximum downhill direction (steepest descent path), although topography, represented by a Digital Elevation Model (DEM), does have a strong impact on the lava inundation results. The DEM prepared for this work (0) is believed to provide enough information about the terrain and the slope to simulate the lava flow accurately, especially on the steeper slopes. As was found during the Holuhraun eruption, the flatter the pre-emplacement topography, the higher the impact of DEM accuracy on the lava flow simulations (Tarquini et al., 2018). A DEM intrinsically contains smoothing of the real surface, and small-scale morphological features that are below the resolution of the DEM, can, at times, have a strong impact on the direction of propagation of long lava flows, especially over flat surfaces.

When running MrLavaLoba, the operator changes parameters that probabilistically influence the lava emplacement, such as where new parcels, or lobes of lava, bud from the previously emplaced lava, and how much the direction of propagation of the parcels of lava can deviate from the maximum downhill direction. We initially tuned the emplacement parameters to the 1973 Eldfell eruption, releasing the total volume of a Moderate sized eruption from Eldfell over

the pre-eruptive DEM. The parameter values that generated simulation results that most closely matched the relocation, length and thickness of the 1973 lava flow were used for the entire suite of Moderate-volume simulations over the post-emplacment DEM. The Small- and Large-volume eruptions required different variable values to optimize the simulated lavas' thicknesses and lengths (Table 2) to replicate the length and thickness of actual lava flows (Table 1). The input parameters used are shown in Appendix B.

The 1973 lava flowed from land into the sea and had observed flow changes due to the interaction with the sea. Because Heimaey is small and lava flows from the Vestmannaeyjar system can be large, lava flows that begin on the land have a good chance of entering the sea, thereby developing as hybrid land/sea lava flows, like the 1973 lava flow. Submarine lava flows have a narrower and weaker outer brittle crust compared with subaerial lava (Mitchell et al., 2008). This promotes irregularly located breakout points of advancing flow. This can result in a greater number of smaller subaqueous flow units having a smaller runout potential, such that a final lava deposit under the sea would be thicker and shorter than an equivalent lava deposit on land. Sea water/lava interactions, however, are not explicitly described by the model, so phreatic explosions, for example, are not accounted for. The simulated lava is essentially emplaced into an empty basin; i.e., there are no changes to the lava emplacement when entering the sea. This implies that the submarine part of lava flows simulated by the model will be longer and thinner than they would be in reality. No attempt has been made to quantify the uncertainties of the simulated lava emplacement thickness and length due to ignoring the role of water. We assume this is within the extremely large uncertainty and variance of lava thicknesses measured in real deposits. Future work analyzing this could be potentially beneficial.

The exact location of the next eruption of the Vestmannaeyjar volcanic system is unknown. Simulations were therefore performed of lava flows originating from over 2000 potential vent locations on Heimaey placed at regular intervals of 80 m (Figure 6). Eighty meters spacing between potential vents was chosen to be a sufficiently high resolution to see differences in lava emplacement based on vent location. The simulated eruptions were treated as though all erupted lava came from a single vent, whereas in reality, lava is erupted from several vents, as was the case during both the Surtsey and Eldfell eruptions. It is common, however, that as an eruption progresses, the eruptive activity coalesces into one main vent, as was the case with the Eldfell eruption. We therefore treat the simulated lava flows as though this latter eruption stage is constant throughout the lava emplacement, because we cannot change from multiple vents to a single vent during a single simulation. This has the impact that the simulated emplacement may be too thick closest to the vent. Vents were only allowed to be on land. In reality, eruptions can originate under water which could grow sufficiently to produce lava flow onto Heimaey. Such conditions were, however, not considered, due to the great uncertainties in such simulations. This means that the hazard of lava flow inundation on the coastal edges of Heimaey are underestimated.

We also do not know how large the next eruption will be, so three eruption sizes, representing Small, Moderate, and Large eruptions of the Vestmannaeyjar system (Section 3.3; Table 2) were used. Each eruption size was simulated to start from each of the potential vent locations. In each simulation, lava that originates from one vent can travel in multiple directions from the vent, and the probabilistic maps will show which directions are most likely. A convergent solution of where lava is most likely to flow from a given vent provides the extent and thickness of the final eruption deposit. In total we performed over 6000 simulations of potential future lava flows on Heimaey.

This probabilistic modeling approach allows us to evaluate how vent location and eruption size can influence the potential impacts of lava flow during future eruptions.

Table 2: Characterization of the three different eruption size scenarios based on volumes in the CIV (Höskuldsson, 2015). “Volume input in model” is an input to the simulations, while thickness and length are results from the optimal tuning simulation for each size eruption scenario.

Eruption scenario	Volume in CIV [km ³]	Volume input in model ⁶ [km ³]	Thickness [m]			Length [km]
			Min	Mean	Max	
Small	<0.1	0.01 ⁷	6	26	53	0.6
Moderate	0.1–0.5	0.13 ⁸	14	47	94	1.6
Large	> 0.5	0.65 ⁹	10	56	149	3.3

The volume of erupted material in these simulations is the volume of lava only as specified by the three size categories shown in

Table 2, while the volume for the eruption sizes provided in the chapter on Vestmannaeyjar in the CIV (Höskuldsson, 2015) is the total erupted volume of material including tephra plus lava. These simulated eruptions begin on land, where more lava is produced and less tephra. The 1973 Eldfell eruption, for example, produced 0.27 km³ lava and 0.02 km³ of tephra. For eruptions that begin on land, we therefore assume that the erupted volumes provided in the CIV are reasonable approximations of lava volumes.

Spatially variable lava inundation probabilities are calculated using the aggregation of all model results for all eruption sizes and vent locations (Figure 6). Places that experienced inundation in a greater number of runs are calculated to be more likely to be inundated than those with fewer inundation outcomes. Eruption location spatial preference is not included in this calculation.

3.3 Potential lava inundation from hypothetical eruptions

The results shown here are from the MrLavaLoba model for the likelihood of lava inundation if there is an eruption on Heimaey. Figure 7 shows the results from an eruption beginning downtown to serve as an example of the full set of over 2,000 potential vent locations considered on Heimaey. This figure shows the on-land distribution of lava flow simulations from Small, Moderate, and Large scenarios.

⁶ Volume in model = lava; Volume in Catalogue = tephra and lava; Höskuldsson, 2015.

⁷ Small scenario volume based on Klif 12900 BP eruption (Mattsson & Höskuldsson, 2003).

⁸ Moderate scenario volume based on the volume from the Eldfell 1973 eruption reported by (Jakobsson et al., 1973). When the simulations were made, the estimate of 0.27 km³ put forth by this work had not yet been calculated. Both 0.13 and 0.27 km³ are within the 0.1–0.5 km³ range for Moderate eruptions.

⁹ Large scenario volume based on Helgafell 5900 BP eruption (Mattsson & Höskuldsson, 2003).

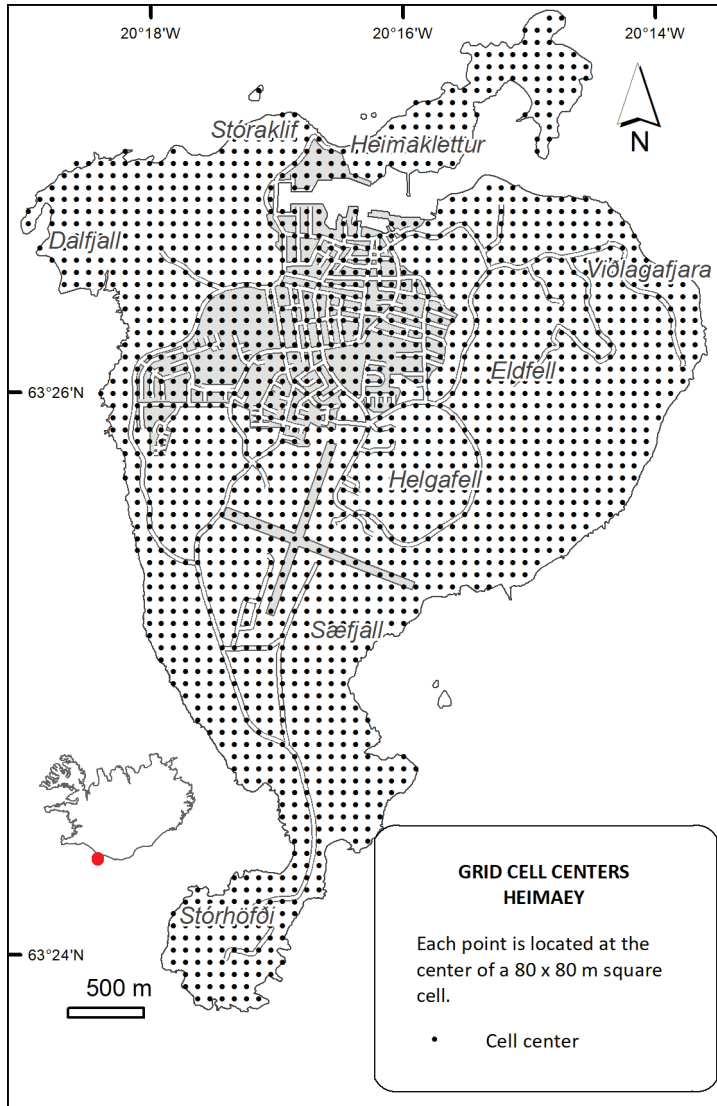


Figure 6: Map of Heimaey showing the regular, gridded locations where modelled lava flows originated.

Figure 7 shows where lava could flow from a single example vent and Figure 8 shows the distribution of modeled lava from all the vents located on an 80 m grid across the island. Figure 9 delineates the areas from where lava flow could impact four defined areas of interest: the harbor, downtown, residential neighborhoods, and the airport. The three outlines encircle the regions where Small, Moderate, or Large lava flows could originate and flow into the area of interest.

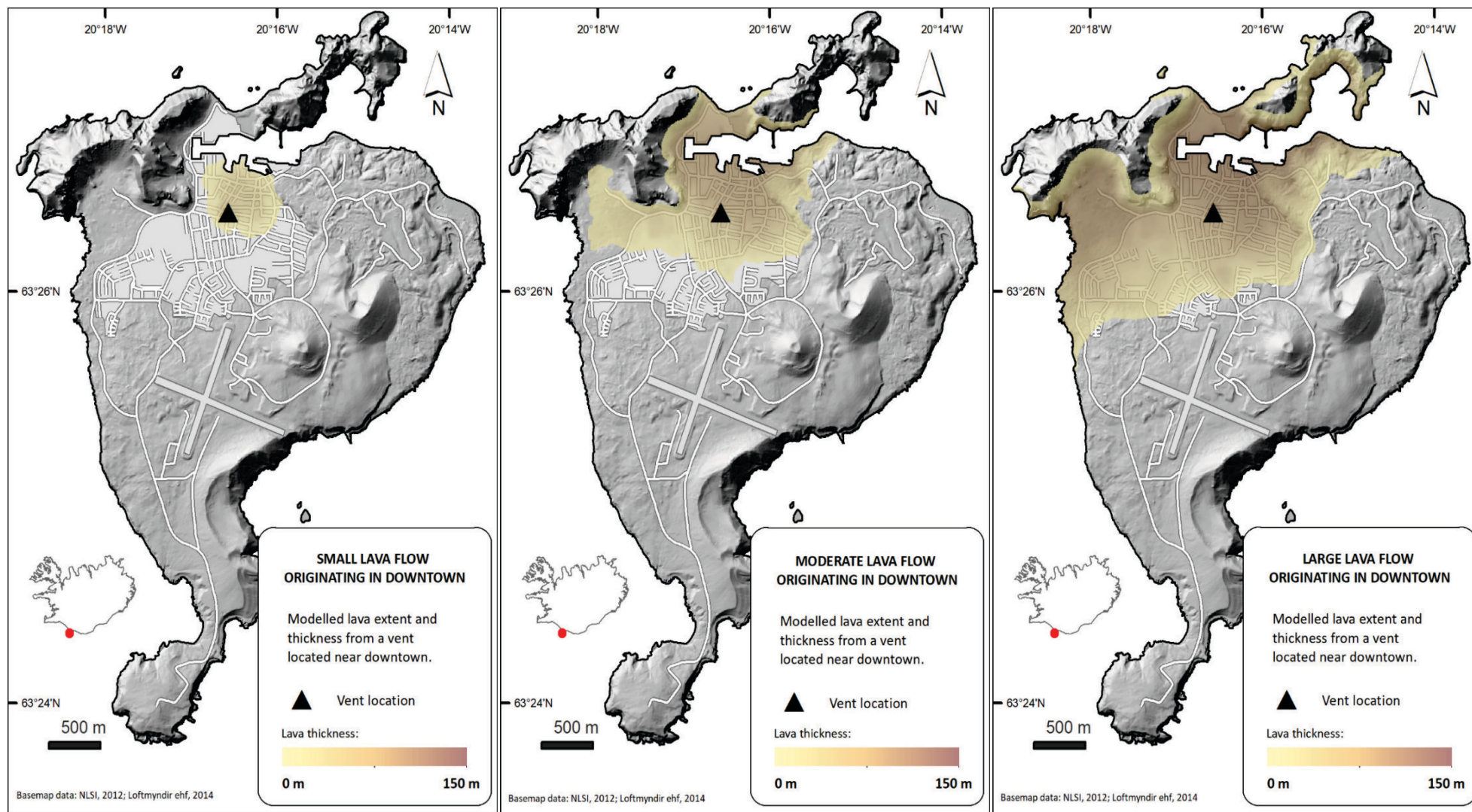


Figure 7: Modeled extent and thickness of lava from Small (left), Moderate (center), and Large (right) eruptions originating from a single vent location in downtown. One of the deterministic simulations used to produce the probabilistic map (Figure 8). Only results on land are shown. The residential areas are shaded in grey.

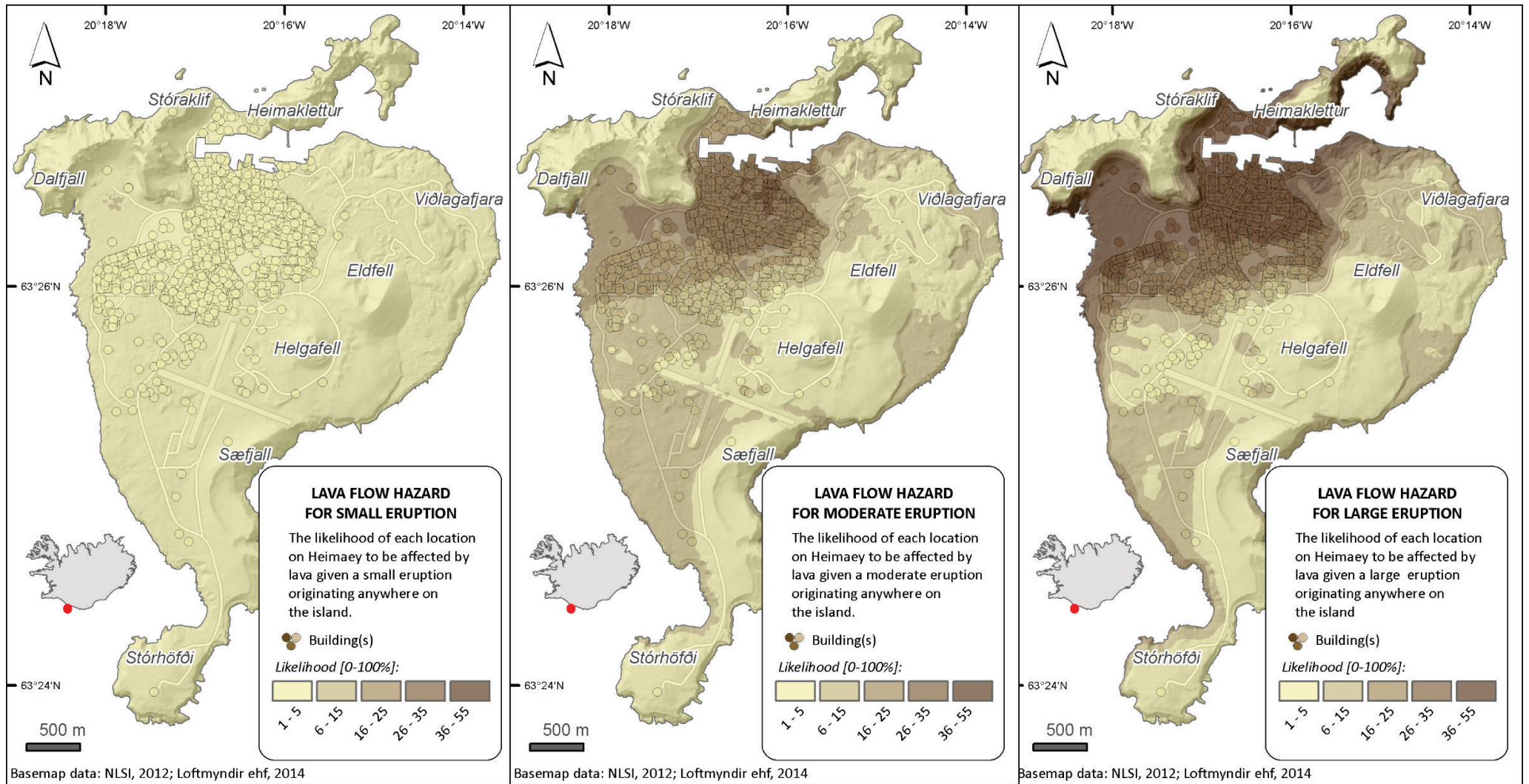


Figure 8: The likelihood that locations on Heimaey will be inundated by lava given a Small (left), Moderate (center), or Large (right) eruption anywhere on the island. All vent locations have equal probability. Buildings are shown as more intense, but the same color as the area they are in. These probabilistic maps are built from the deterministic simulations of which one example is provided in Figure 7.

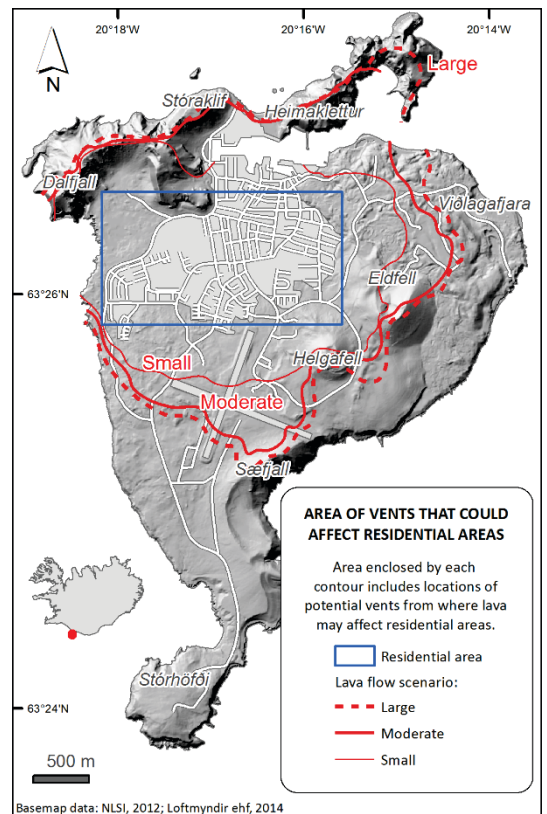
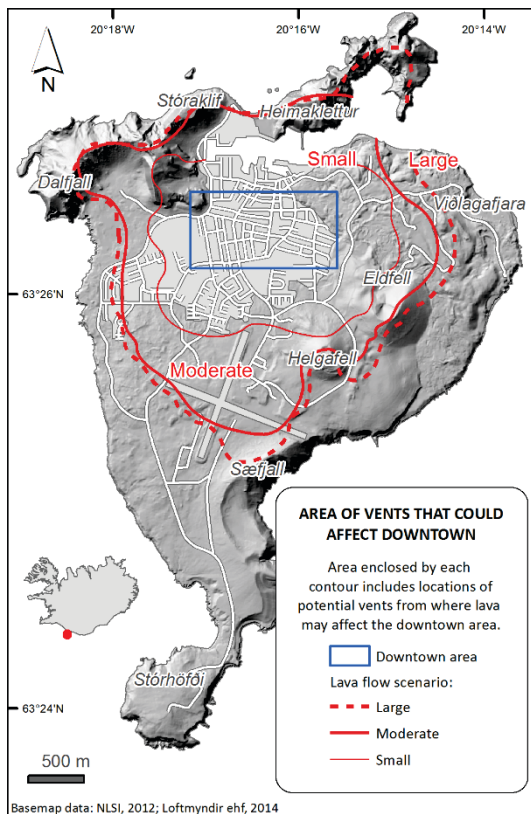
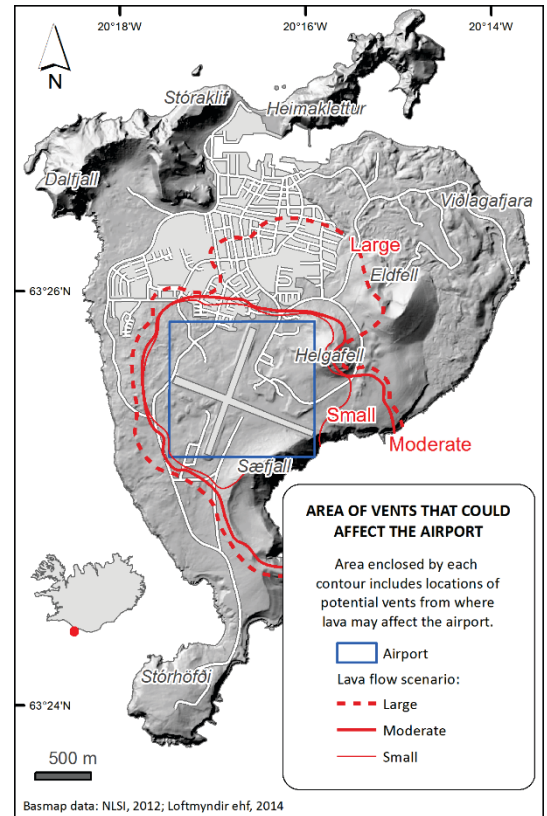
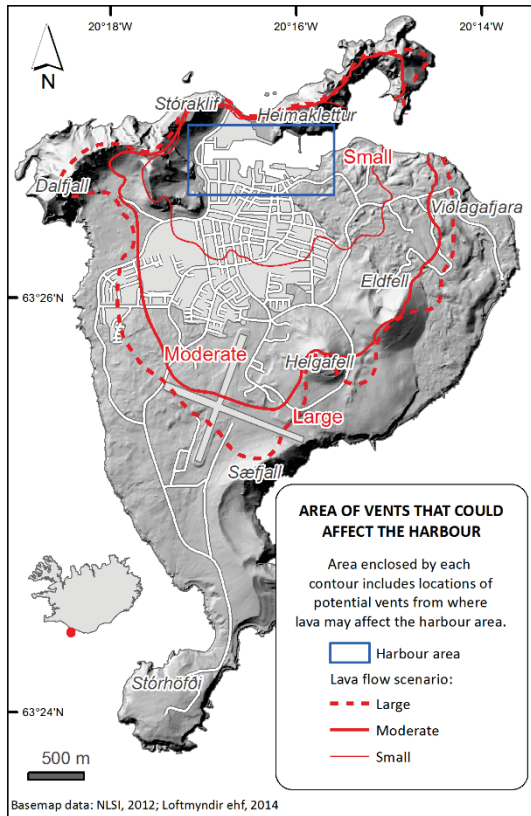


Figure 9: Areas where eruptions could originate whose lava could impact areas of interest (blue box): harbor (top left), airport (top right), downtown (bottom left) and residential areas (bottom right). Small eruption area encircled by a thin solid line, Moderate eruption area encircled by a thicker solid line, and Large eruption area encircled by a dashed line. The residential areas are shaded in grey.

3.4 Tephra mass loading

“Volcanic tephra” refers to all the pyroclastic material injected into the atmosphere during an eruption. Tephra include ballistics/bombs (everything larger than 64 mm in diameter), lapilli ($2\text{ mm} < d < 64\text{ mm}$) and ash ($d < 2\text{ mm}$) (Wolff & Sumner, 2000; Table 3). Due to its small size, ash can persist in the atmosphere for days and weeks and be transported far away from the eruptive source, whereas lapilli and bombs have an impact closer to the vent.

Table 3: Terminology used in the report for pyroclastic material and its size.

Term	Size
Ballistic/Bomb	$d > 64\text{ mm}$
Lapilli	$2\text{ mm} < d < 64\text{ mm}$
Ash	$d < 2\text{ mm}$
Fine ash	$d < 0.063\text{ mm}$

Damages caused by tephra loading, including only the lapilli and ash size fraction, have been investigated using a numerical model. We use two different vent locations for the tephra simulations. Probabilistic analyses of the model results were used to identify the most exposed places and infrastructures on the island to tephra mass loading. We examine the model results with regards to established impact thresholds for specific threats to infrastructure if no mitigating actions are taken. The fire hazard from hot tephra landing on or in buildings, as happened during the 1973 eruption and can be anticipated to happen during future eruptions, was neglected in this work. This hazard will be particularly benefited by mediation actions taken during an ongoing eruption.

3.5 Tephra dispersal and deposition model

The VOL-CALPUFF tephra dispersion and deposition model is an expansion of the CALPUFF model that was developed to reproduce some processes specific to volcanic eruptions, such as the plume rise phase of an eruption and the release of solid particles (Barsotti et al., 2008). This model has been used to reconstruct past tephra-producing events at many volcanoes around the world and in Iceland, including Eyjafjallajökull 2010 (Spinetti et al., 2013), Grímsvötn 2011 Öræfajökull 1362 (Barsotti et al., 2018) and in the “Volcanic hazard assessment for explosive eruptions in Iceland – Sprengigos á Íslandi”, a GOSVÁ project, to create volcanic tephra hazard maps for Hekla, Katla, and Öræfajökull (Barsotti et al., 2020). We chose to use this model here because of the focus on proximal hazards. VOL-CALPUFF models small-scale atmospheric dynamics, including localized wind shears, boundary-layer dynamics, diurnal weather variations, and different forms of precipitation to affect the dispersion and deposition of the tephra. VOL-CALPUFF’s plume-rise and localized wind features are particularly important for simulating tephra dispersion and deposition close to an eruption source. The VOL-CALPUFF model calculates the hourly deposition of tephra as ground load in kg/m^2 .

The VOL-CALPUFF model was used to simulate moderate subaerial eruptions (like the 1973 eruption) from two vent locations: at Eldfell and at Surtsey. These were chosen to represent eruptions of the Vestmannaeyjar system proximal and distal to Heimaey. To represent the statistical variability of the meteorological conditions, which governs the tephra dispersal and deposition, a Monte Carlo approach was used. A random sample from ten years of meteorological data (including the years 1980–1991) from the European Centre of Medium-range Weather Forecast (ECMWF) was used in each run. VOL-CALPUFF generates a refined analysis of the atmospheric properties.

Each run simulated a six-day-long eruption and calculated the tephra ground load over a grid with 50 m spacing. The eruption source parameters (ESP) used as input to the dispersal model were constrained based on plume heights and deposit thicknesses of the 1973 Eldfell eruption (Table 4). The best fit between simulation results and measurements made during the eruption was obtained by using a variable mass flow rate of the mass erupted during the first six days of the eruption based on the isopach map shown in Figure 4 in order to reproduce column height variations (Figure 10). Tephra generation was episodic in 1973. Regardless of if the temporal changes were due to phreatomagmatic activity or changes in the magmatic gas content, within the model, the variation of the mass flow rate is adequate to produce a variable tephra production over the duration of the simulated eruption.

Some properties of the 1973 eruption dynamics and of the volcanic cloud mixture are provided in Table 4. They have been used as reference values to set up the initial eruption conditions in the model. The values used as input to the model (bold values in Table 4) are best fit values to reproduce the 1973 eruption observations. A gas mass fraction significantly higher than the up to 1 wt% typical of Icelandic eruption products (e.g., Jamtveit et al., 2001; Nichols et al., 2002) was used to characterize the volcanic mixture in the model.

The total grain size distribution used for the simulations is shown in Figure 11. The histogram shows that the size of tephra simulated with VOL-CALPUFF includes lapilli and ash only. Bombs and ballistics are here not considered as the model does not account for ballistic trajectories in its physics.

Up to 400 runs were performed until the probability of exceeding specific thresholds in the ground deposit converged to a stable result.

This probabilistic modeling approach allows us to evaluate how eruption location and weather conditions influence the potential impacts of mass loading from tephra deposition during future eruptions.

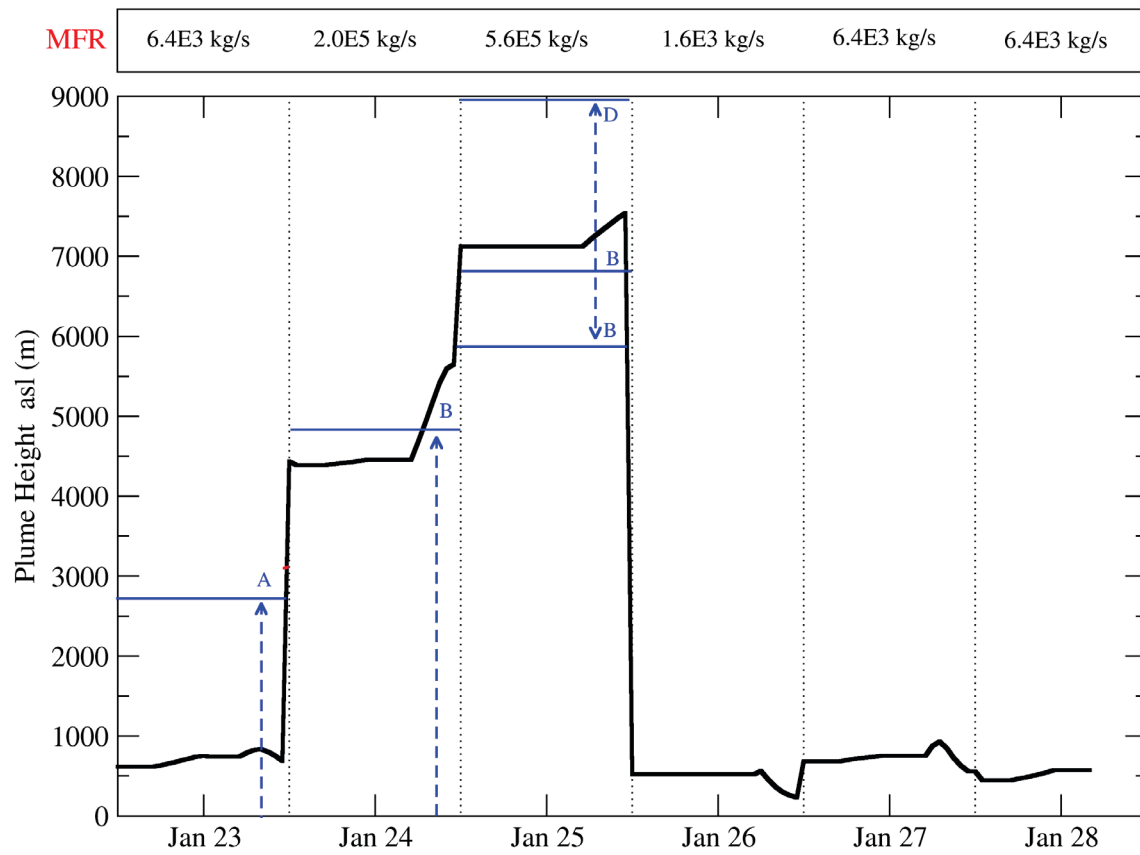


Figure 10: Daily maximum plume heights observed during the 1973 eruption (blue lines). Letters refer to references provided in Table 4. Time series of plume height (continuous black line) produced by the VOL-CALPUFF model simulation of the first six days of the 1973 eruption. The mass flow rate (MFR) used for each day of the simulation, chosen by trial and error to achieve the simulated plume heights, is written above the plot.

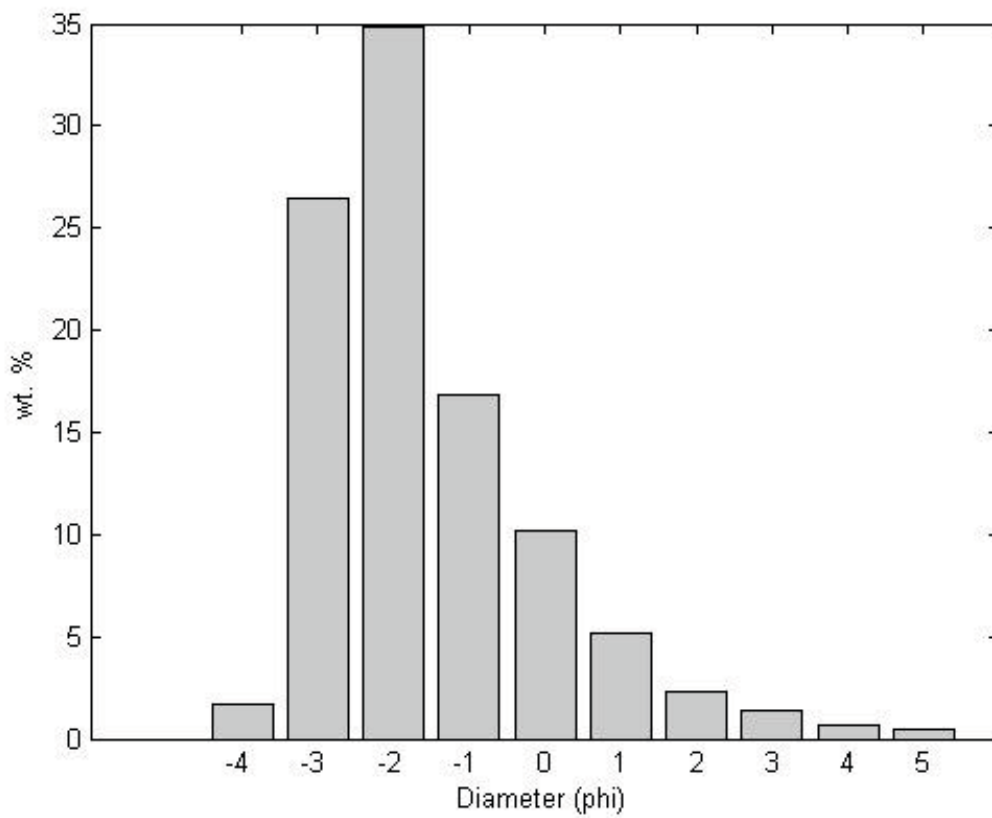


Figure 11: Total grain size distribution of lapilli and ash measured during the 1973 Eldfell eruption. Diameter in phi is equivalent to the following in mm: -4 ϕ = 16 mm; -3 ϕ = 8 mm; -2 ϕ = 4 mm; -1 ϕ = 2 mm; 0 ϕ = 1 mm; 1 ϕ = 0.5 mm; 2 ϕ = 0.25 mm; 3 ϕ = 0.125 mm; 4 ϕ = 0.0625 mm; 5 ϕ = 0.0312 mm. The total grain size distribution calculation is described in 0.

Table 4: Eruption source parameters measured in the 1973 Eldfell eruption (top row) and used to constrain input to the model (bold) and model results (not bold) (bottom row). First column is displayed graphically in Figure 10.

	Max. plume height [km]	Erupted mass tephra [kg]	Tephra density [kg/m ³]	Vent diameter [m]	Magma temp. at vent [C]	Exit velocity [m/s]
1973 Eldfell eruption ¹⁰	2.7 ^A , 4.8 ^B , 5.8 ^B , 6.7 ^B , 9 ^D	1.1E10 ^E	533 ^F	20 ^G	1055 ^C	92.5 ^F –157 ^G
Simulation of Moderate scenario ¹¹	0.6, 4.7, 7.1, < 1	5.2E10	533	6–50	1028	90–150

References: A: Sigurðsson, 1973; B: Sigurdsson, 1973; C: Jakobsson et al., 1973; D: Thorarinsson, 1973; E: Williams & Moore, 1976; F: Self et al., 1974; G: Blackburn et al., 1976.

¹⁰ Dates that the maximum plume heights were observed (all 1973). 2.7: 13 March; 4.8: 24 January; 5.8: 25 January; 6.7: 25 January; 9.0: 25 January.

¹¹ Höskuldsson (2015) considers a Small subaerial eruption unlikely and advise that a Moderate subaerial eruption and a Large subaerial eruption could produce a maximum plume height of <4 km and <10 km, respectively.

3.6 Potential tephra deposition from hypothetical eruptions

A place-based hazard analysis was made of tephra load in downtown Heimaey. The worst case (most tephra deposited) was produced using meteorological conditions starting on 2 September 1984 (Figure 12, left) and the best case (least tephra deposited) was produced using meteorological conditions starting on 9 January 1984 (Figure 12, right). These are two of the deterministic simulations used in the probabilistic analysis. The vertical profiles of the wind speeds and wind directions extracted at the grid point closest to Eldfell for the two simulations are shown in Figure 13. During the first two days of the worst-case eruption, the wind direction blows from north and east. In particular on the second day, the wind blows from the east at all altitudes up to 15 km. In the best-case scenario, the wind blows from almost any direction close to the surface, but it is consistently blowing from the west-southwest above 5 km. The wind speed in the worst-case scenario is much lower than during the best case for the first two days of the eruption (~10 vs 30 m/s at 5 km). All these elements explain why for the worst-case scenario the highest deposition is downtown, and the affected area is spread over all the island (the peak downtown is ~550 kg/m²). In contrast, in the best case the peak is much farther from the vent and most of the island is free from tephra fallout (the peak downtown is ~0.008 kg/m²).

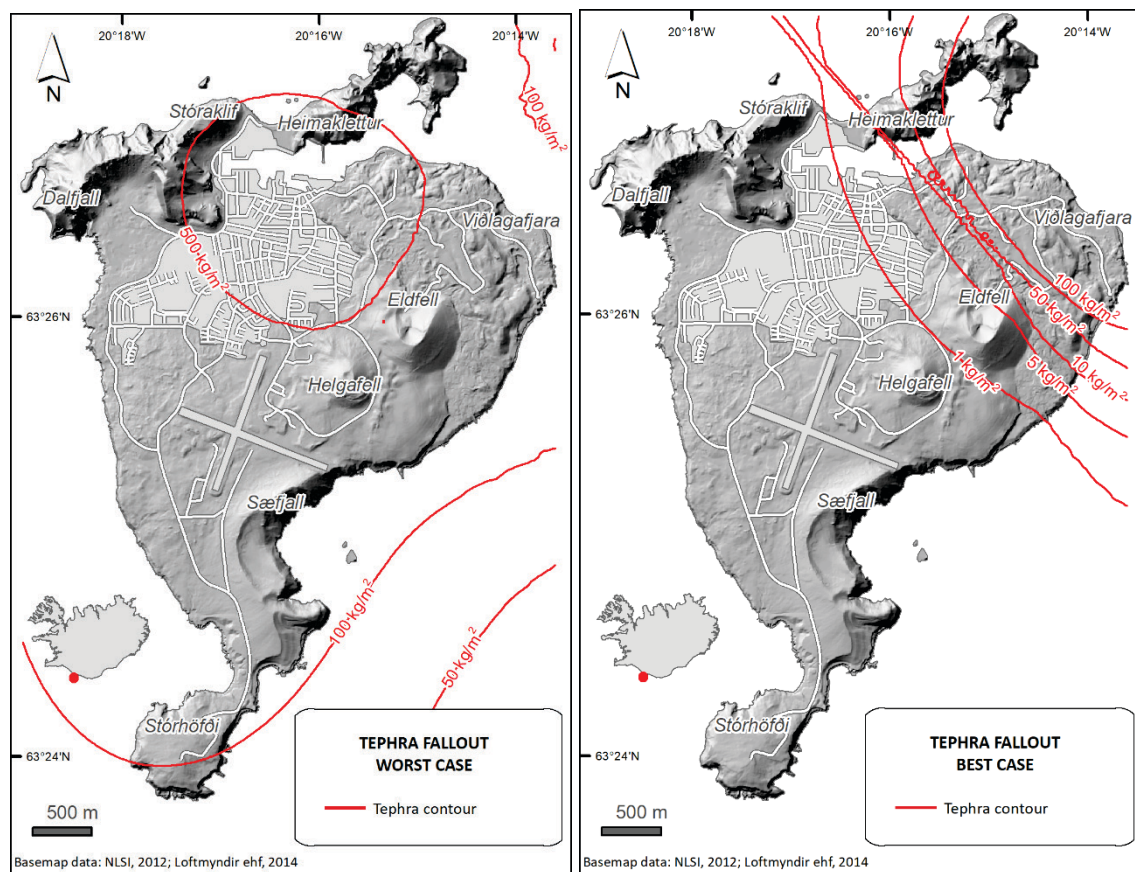


Figure 12: Moderate sized eruptions with six days duration from a vent at Eldfell. Simulations were made using meteorological conditions from ten years of data. The worst-case simulation is that resulting in the greatest amount of tephra in downtown was produced using meteorology starting on September 2, 1984 (left) and best-case simulation produced using meteorology starting on January 9, 1984 with the least tephra deposited in downtown (right). The residential areas are shaded in grey.

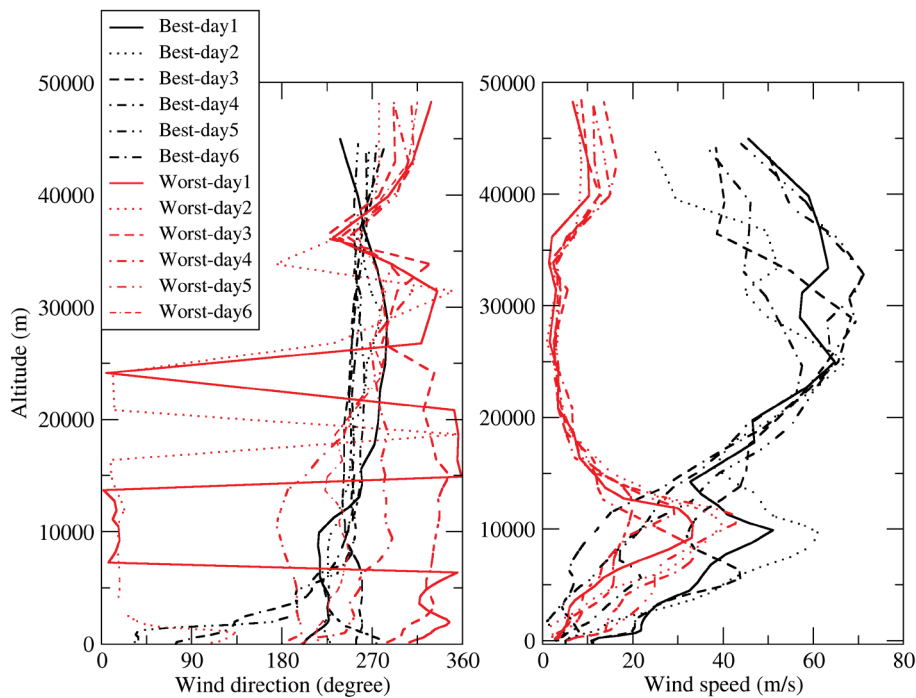


Figure 13: Vertical profile of the wind direction (left) and wind speed (right) for the worst case (red) and best case (black) simulations extracted at the grid point closest to the vent shown in Figure 12.

A probabilistic analysis of tephra deposition was made. The load exceedance probability is calculated by dividing the number of simulations for which a specific tephra load was exceeded by the total number of deterministic simulations (two examples provided in Figure 12). The places with the highest probability are more exposed to potential tephra deposition. We have plotted the exceedance likelihood of deposits using an arbitrary threshold of 30 kg/m^2 , which is equivalent to a dry deposit thickness of 3 cm, to illustrate where tephra is most likely to be deposited during an eruption at Eldfell (proximal to Heimaey) or Surtsey (distal to Heimaey) (Figure 14, left and right, respectively).

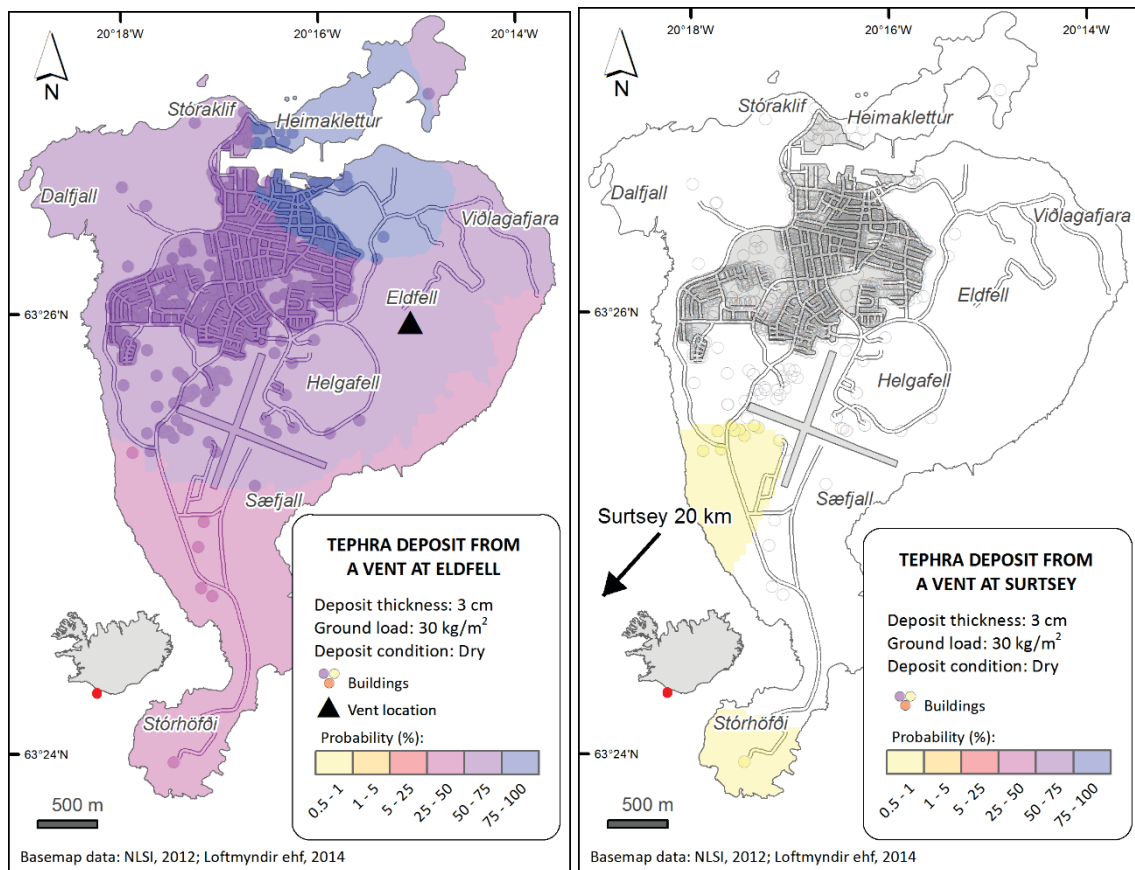


Figure 14: The probability that tephra (<64 mm) released from a six-day long Moderate eruption at Eldfell (left) and Surtsey (right) would form a 3 cm thick deposit on Heimaey. Ten years of meteorological data are used to produce this probabilistic solution. Buildings are shown as more intense, but the same color, as the area they are in. The residential areas are shaded in grey, which changes the hue of the color scale.

There is, as expected, much more tephra deposited on Heimaey when an eruption of the Vestmannaeyjar system originates on the island itself. A Moderate eruption from Surtsey has a very small likelihood of accumulating 3 cm of tephra on Heimaey (less than 1% everywhere on the island). Given a hypothetical Moderate eruption located at Eldfell in the northeastern part of the island, tephra is more likely to be deposited towards the north across the island.

The accumulation of tephra is dependent upon column height due to vertical variations in wind direction and velocity. Wind rose diagrams show wind direction and speed for six elevations using the 10 years of ECMWF meteorological data from the point closest to Eldfell (Figure 15). These wind rose diagrams show that closer to the ground, at 1000 hPa, the wind is weaker than at higher elevations and prevailing winds blow from easterly directions. At 850 hPa, which is approximately 1,500 m elevation, similar to the lowest observed maximum plume heights during the 1973 eruption, the wind blows predominantly from the SSW. By 300 hPa, or approximately 9,000 m, similar to the highest of the maximum plume heights observed during the 1973 eruption, there is an even stronger westerly component. The wind becomes stronger at higher altitudes. For a hypothetical eruption located at Eldfell, based on this statistical analysis, as an eruption reaches its maximum possible intensity (highest maximum plume height) its tephra would be less likely to be deposited on Heimaey, while weaker eruptions would be more likely to deposit their tephra on the island.

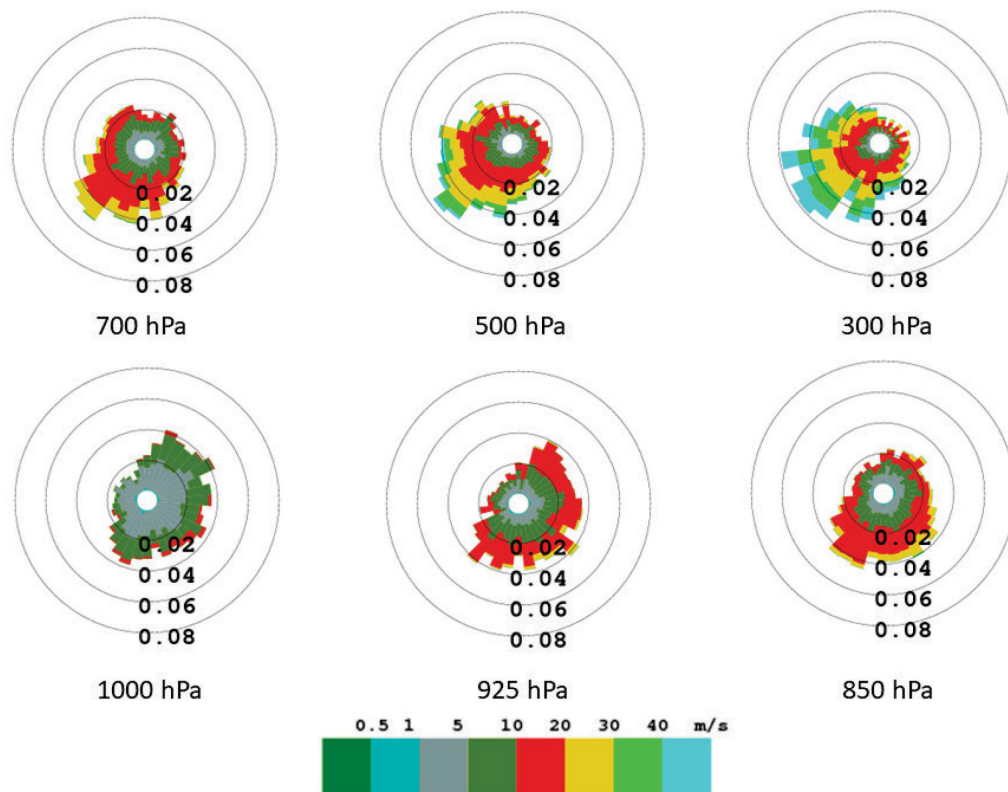


Figure 15: Frequency of wind direction and wind speed shown for six different pressure levels and corresponding elevations: 1000 hPa ~ 100 m a.s.l.; 925 hPa ~ 750 m; 850 hPa ~ 1500 m; 700 hPa ~ 3000 m; 500 hPa ~ 5600 m and 300 hPa ~ 9000 m.

3.7 Modeled locations of potential future eruptions

The location of the next eruption of the Vestmannaeyjar volcanic system is unknown, but the relative spatial probability of vent opening can be estimated based upon the locations of mapped vents (e.g. Selva et al., 2012). The bathymetry around the Vestmannaeyjar archipelago has been mapped (Figure 2) where bathymetric rises are related to volcanic deposits and volcanic mounds are inferred to be subaqueous vents based on morphological criteria alone (0). We calculate relative spatial vent opening probability in the volcanic system within the area covered by the bathymetric data (Figure 2) such that the sum of all the probabilities within the domain is 1 (or 100%). The probabilities were computed on a grid of 400 m x 400 m, which provides satisfactory resolution over the size of the domain. We have not calculated absolute likelihood of eruption but present the spatial likelihood conditional upon an eruption: where vent opening is more likely to occur. We use two different methods to model vent opening probability distribution: 1. Assigning a normal distribution to vent position about a single linear axis and 2. Using a Gaussian kernel-smoothed function to approximate spatial clustering of vents. Because the ages of the submarine features are so poorly understood, both models consider only vent locations, but not inferred vent ages.

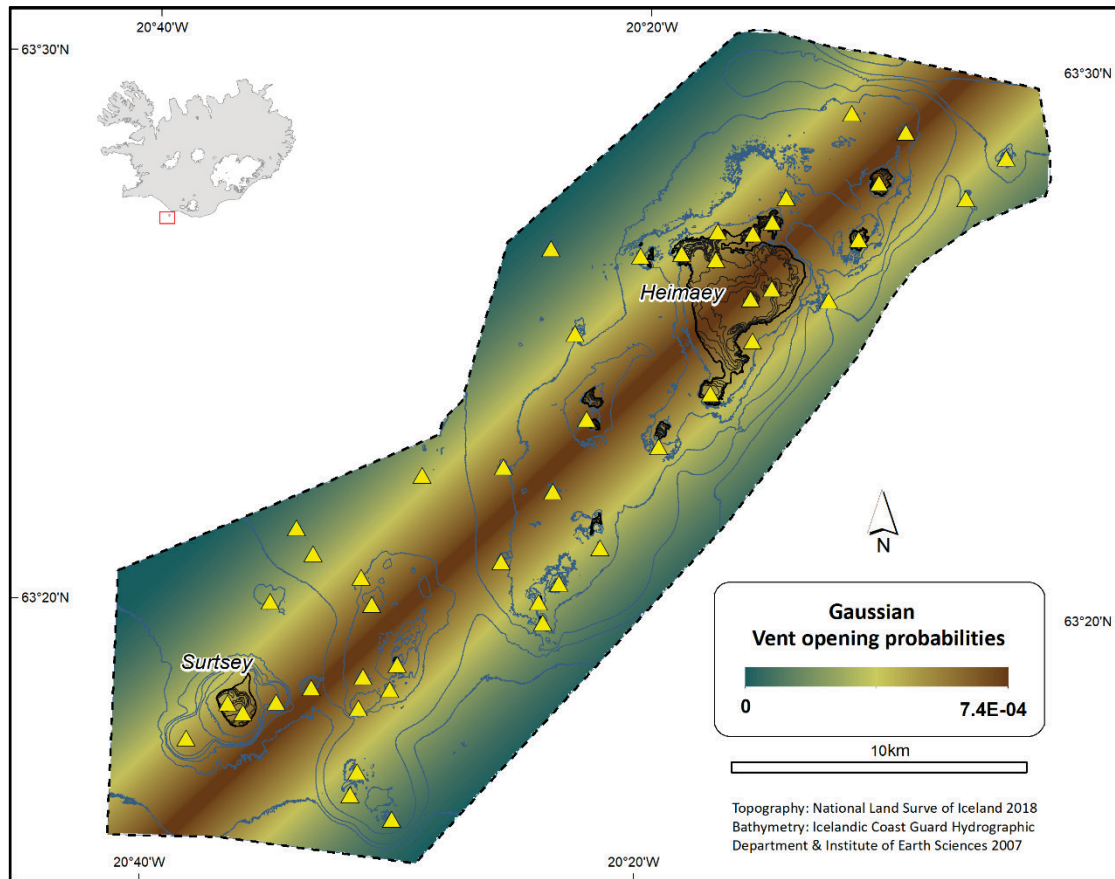


Figure 16: Probability of location of future vent opening based on the best fit line of the identified previous vents using a normal distribution. One standard deviation = 2.5 km. Past vents are indicated by triangles. The sum of the probabilities within the domain is 1 (or 100%).

As there is relative spatial symmetry to the best fit line of the mapped vents (Appendix D), a simple model for future vent openings was calculated and will be referred to as “normal distribution”. Based on this relationship, the highest likelihood of future vent openings is along the best fit line of previous vents and the likelihood decreases with distance from this line (Figure 16). This orientation line follows the trend of the eastern volcanic zone, is parallel with the fissure swarms of the EVZ (Figure 1), and within the main part of the Vestmannaeyjar fissure swarm as drawn by Jóhannesson and Sæmundsson (1998) (Figure 1). While several eruption fissures have opened along this same orientation (including Elliðaey, Bjarnarey and Surtsey; Jakobsson, 1968), there are also en echelon tension gashes oriented obliquely to this orientation (including Surtur II and the fissures of the Heimaklettur formation; Jakobsson, 1968). Additionally, the bathymetric map (Figure 2) shows parallel topographic ridges oriented oblique to the vent trend as is seen in other rift systems, e.g. the Reykjanes ridge. The normal distribution model ignores the increased likelihood of vent opening along these oblique tectonic sections. It also ignores the possibility that there may be more than one line along which future eruptions may be more likely to occur, such as proposed in (Jakobsson, 1979) and the possibility that volcanism may be preferred around Heimaey, as would be the case if a central volcano is developing (Mattsson & Höskuldsson, 2003). Age variation of the vents is ignored as is discussed in 0. Perpendicular to the best fit line, Heimaey is at the widest about 3.5 km, so this model of future vent locations is regionally coarse relative to specific locations on the island.

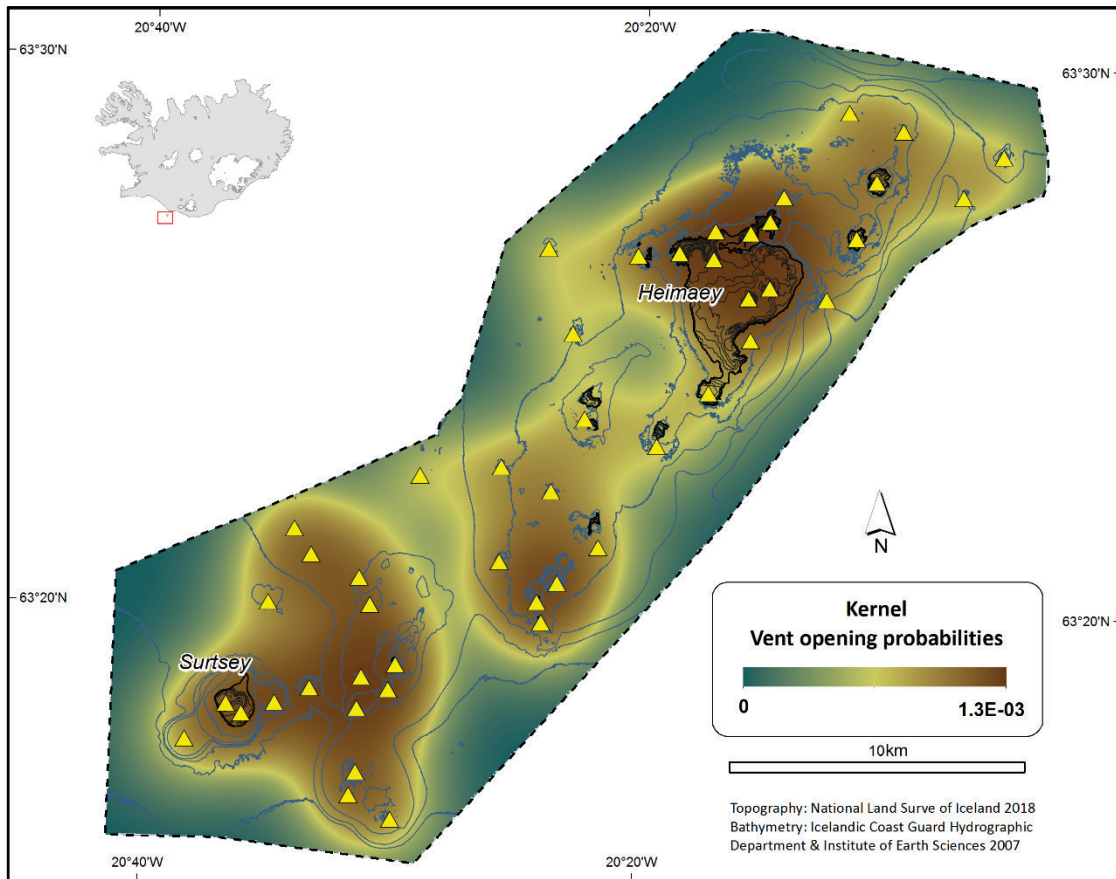


Figure 17: Probability of location of future vent opening based on the locations of identified previous vents using a Gaussian kernel-smoothed function model. Triangles indicate identified past vents. The optimal coefficient of smoothing = 1.5 km. The sum of the probabilities within the domain is 1 (or 100%).

An alternative, widely used model (Martin et al., 2004) is based on the assumption that the next vent location can be forecasted based on the location of past vents. This model ignores the role of the alignment of the volcanic system that is emphasized in the normal distribution model around the best fit line described previously (Figure 16). As with the previous model, it does not incorporate possible spatial dependence on erupted volume or age of the mapped vents.

To develop this model, which will be referred to as the “Gaussian kernel-smoothed function”, an equation is applied to each grid cell to calculate the likelihood that that location (that grid cell) may be the location of the next vent. The probability of the next vent opening at that location depends on a smoothing coefficient “ h ” and the distance of that location to each of the 47 identified vents. The coefficient of smoothing, h , is assumed to be constant over the entire domain, and is calculated using the method of Martin et al. (2004). The choice of the smoothing coefficient has a large impact on the model results, and it depends on several factors including the size of the volcanic system and the degree of clustering of vents. The smaller (narrower) the smoothing factor, the higher the modeled likelihood of future vents being located near past vents, whereas the larger the smoothing factor, the more spatially homogenous the model forecast becomes. To select the optimal smoothing value for the present data set, h was increased stepwise. The distance to the nearest neighbor volcanic vent for each identified vent as seen on the map (real data) was plotted versus the fraction of potential volcanic vents within

the domain that are that same distance to the nearest neighbor (model results). The h value that provided the best match between the real data and the model results is 1.5 km. The Gaussian kernel-smoothed function model for vent opening during the next eruption is shown in Figure 17. This model increases the probability of future volcanic eruptions close to clusters of previous events, independent of their ages.

Both models, normal distribution and Gaussian kernel-smoothed function (Figure 16 and Figure 17), are plausible, justifiable initial models for estimating the most likely locations of the next vent opening in the Vestmannaeyjar system. We do not have enough information to prefer one model over the other and therefore treat both as equally plausible. Both models, as well as an “unweighted model” (i.e. all locations are equally likely, so no weighting is used in the following steps), are used to calculate a range of potential impacts from the next postulated eruption. This does not include any assessment of the absolute likelihood of an eruption occurring within the Vestmannaeyjar system (i.e. an annual probability of eruption). We make no attempt to forecast when the next eruption may occur. In order to do this, it will first be necessary to gain more precise information about the ages of the existing vents.

To summarize, the lava impact calculations were made:

- 1) Assuming no regional preference for where the next vent may open “Unweighted”. All potential vents in the Vestmannaeyjar system, and therefore on Heimaey, are equally likely. As Heimaey is 3% of the area of the domain, this implies a 3% likelihood of the next vent opening on Heimaey (Figure 2).
- 2) Using the normal distribution model around the best fit line through the locations of identified previous vents, to forecast where in the volcanic system vents may be more likely to open. This model estimates a 5% likelihood of the next vent opening on Heimaey (Figure 16).
- 3) Using the Gaussian kernel-smoothed function model based on the locations of identified previous vents, to forecast where in the volcanic system vents may be more likely to open. This model estimates an 8% likelihood of the next vent opening on Heimaey (Figure 17).

With the assumption that there is a 100% likelihood that the next vent opening in the Vestmannaeyjar system will open within our model domain, based on the two likelihood models and the unweighted model, there is a 3–8% likelihood of the next vent opening on Heimaey/92–97% likelihood of the vent opening not being on Heimaey.

4 Exposure

4.1 Critical infrastructure

A dataset from Registers Iceland that features the locations, facility type, and fire-insurance values of infrastructure was used to calculate the vulnerability of infrastructure on Heimaey to tephra and lava hazards in future eruptions (see Table 7 and 8 in Appendix F). The classification system used is the IST120:2012 prepared by Icelandic Standards. This system is based on the Land-Based Classification Standard (LBCS) whereby different types of structures are assigned descriptive codes. The residential building stocks, ~2000 homes, represent the greatest part (64%) of the total economic value of infrastructure on the island. The total value of building infrastructure, using November 2017 values, is 110 billion ISK of which 71 billion is residential buildings.

4.2 People

As of 1 October 2021 there were 4408 residents attached to the Vestmannaeyjabær municipality (Þjóðskrá Íslands, 2021). The people who work on fishing vessels and other temporary workers are variably present on Heimaey and can be initially estimated to be about 150 people. In 2016, 54,000 Icelandic residents and at least 115,000 foreign tourists visited Vestmannaeyjar (Guðmundsson, 2016). The number of people on Heimaey who may need to be evacuated in case of an eruption varies significantly in relation to the time of day and season. The total number of visitors has been increasing annually for all the years 2004–2016. There are strong monthly differences in the number of foreign tourist visitors (Figure 18) (Guðmundsson, 2016, 2018). This dataset indicates that daily visitors may increase the population by up to 30% in July and even up to 50% on specific days and even higher during festivals. In addition to the typical numbers of visitors, Icelandic resident visitors come in very large numbers for four different weekends: Þjóðhátíð during the first weekend in August, Verslunarmannahelgi (approx. 18.000 visitors), soccer competitions for girls, Pæjumót (3.000) and boys, Orkumót (3.000), and the annual celebration of the end of the 1973 Eldfell eruption, Goslokahátíð (5–6.000) (Íris Róbertsdóttir personal communication, 2021). Volcanic unrest during these popular events would affect mitigation actions. This means that the risk mitigation planning should consider the time of day and time of year when the volcanic unrest may occur. Daytime versus nighttime and summer versus winter may have a tremendous impact on the number of potentially vulnerable people (Pagneux, 2015), and weather conditions can have a big impact on the possibilities for sea travel evacuation. The short visits by most of the foreign tourists also mean that the potential for educating them on how to behave in case of volcanic unrest is quite limited.

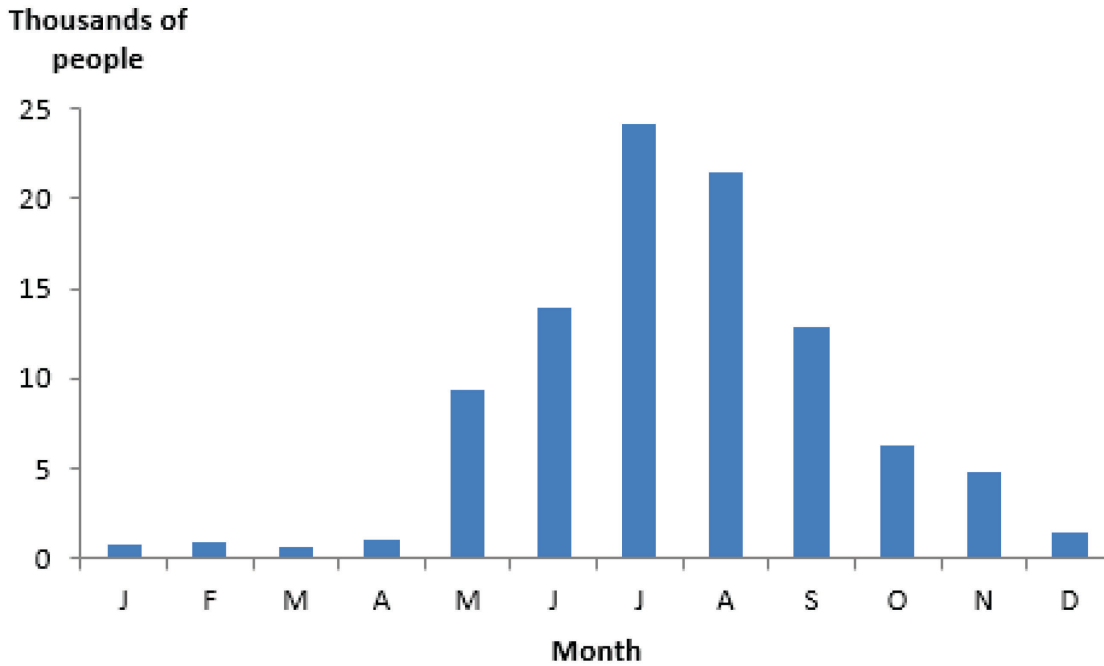


Figure 18: Monthly foreign visitors to Heimaey in 2016, excluding Icelandic residents and visitors from cruise ships. All data from Guðmundsson (2016).

5 Impacts

5.1 Lava inundation

For the Small, Moderate, and Large eruption scenarios simulated in this work, the likelihood of lava inundation in any given place increases as the size of the eruption increases (Figure 8). The southern parts of the island are least likely to be inundated by lava. The most densely populated parts of Heimaey have the greatest likelihood of being inundated by lava if a vent opens on Heimaey because of their location in areas of low topography. The regional vulnerabilities to lava inundation become more pronounced with increased lava volume. This is seen in Figure 9 where Moderate (area enclosed within the thicker solid line) and Large (dashed line) scenario eruptions from most parts of the island produce lava flows that can inundate the harbor, downtown, and the residential neighborhoods. The highlighted individual scenarios are cropped to show only results on land. It is shown that an eruption originating in downtown (Figure 7) would flow north towards the harbor and southwest through the residential neighborhoods. An eruption originating in the northeast of Heimaey could impact the harbor (not shown). An eruption originating near the airport would flow towards the residential neighborhoods, and if the volume was sufficiently large, the lava could inundate downtown and the harbor (not shown).

5.2 Tephra fall

Volcanic tephra can severely affect infrastructure and services that are relied on daily for the social and economic life of a community. Within this project, we focused on the direct impacts of tephra fallout on critical infrastructure that could cause serious disruptions to the local

population. Cascading effects, where damage to one element of infrastructure leads to further disruptions, are not discussed here. Exceedance probabilities for tephra accumulation and mass burden thresholds from eruptions at Eldfell or Surtsey are shown in the subsections below. Mass burden results are presented as two endmembers, for completely dry tephra (there was no precipitation during the eruption) and fully water-saturated conditions. The simulations are performed as though the eruption takes place under dry conditions. The model provides mass loading, and we assume a deposit density of 1000 kg/m^3 which allows us to calculate a thickness of dry tephra deposit.

5.2.1 Roads and airport runways

Volcanic tephra on roads and airport runways can cause reduction in tire friction, obscure road markings, cause blockage of engine air intake filters, and reduce visibility. Laboratory experiments investigating the tephra thickness, presence of precipitation, tephra composition, and particle sizes and how these factors influence how tephra affects skid resistance found that dry tephra deposits on roads between 1–5 mm thick can be hazardous (Blake et al., 2017). This impact of reducing skid resistance is found to be less pronounced on concrete airport runways than on roads, however as described in Guffanti et al. (2009), tephra can be hazardous at airports due to loss of visibility, communication and electrical system disruption, ground service disruption, and damage to building and aircraft.

Skid hazard is approximated using modeled likelihood of tephra deposition with a thickness of 0.1–0.5 cm on Heimaey due to an eruption from vents at Eldfell or Surtsey (Figure 19). Most roads and the airport runways have a greater than 5% probability of tephra accumulation within this range if the eruption vent is located at Eldfell (Figure 19, left). Interestingly, if the eruption vent is located at Surtsey, almost the entire island would have greater than 5% probability of this critical range being reached (Figure 19, right). This suggests that the impacts of tephra deposition on roads and airport runways on Heimaey should be considered for all eruptions of the Vestmannaeyjar system regardless of vent location. Tephra deposits from mainland eruptions might also be relevant in this range; however, this has not been examined within this work.

5.2.2 Mass loading on buildings

An analysis of the load bearing capacity of residential roofs in Heimaey was made in order to determine appropriate load thresholds for vulnerability assessments (Appendix E). Fifty percent of the residential roofs in Heimaey can be anticipated to collapse at a mass loading of 588 kg/m^2 ; the other half would be expected to withstand this mass loading without collapsing. Probabilities of exceeding 588 kg/m^2 due to a simulated Moderate eruption with its main vent at Eldfell are shown for dry and wet (fully saturated) tephra in Figure 20, left and right, respectively. Estimates of load in dry conditions are taken directly from model results. To calculate the potential mass loading of the wet deposit, the porosity of the dry deposit is used to calculate the void space that can be filled by precipitation falling after the end of the eruption. The weight of water plus dry tephra, when the pore spaces within are fully saturated, provides the mass loading of the wet deposit. Dry and fully saturated tephra are two endmembers; it is most likely that the total mass of tephra plus potential precipitation would be in between these two values.

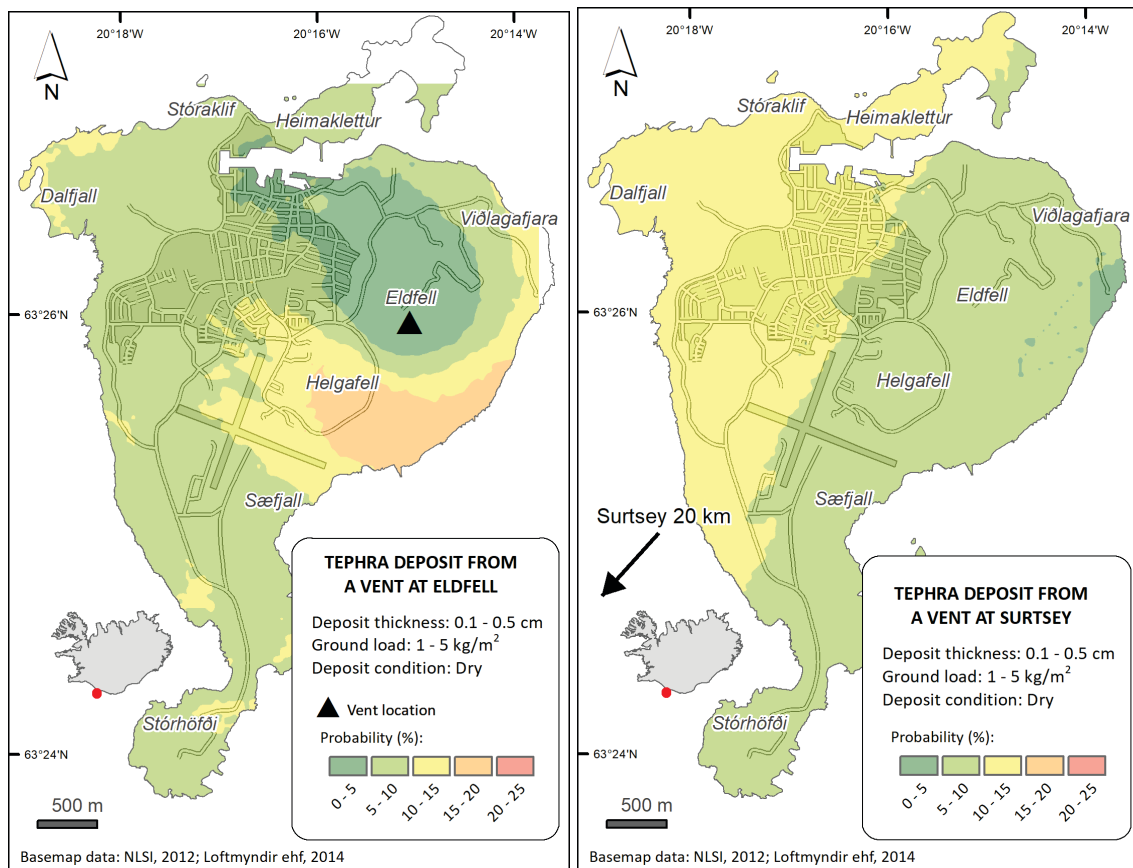


Figure 19: The probability that tephra released from a six-day-long Moderate eruption at Eldfell (left) and Surtsey (right) would form a 0.1–0.5 cm thick deposit on Heimaey. Ten years of meteorological data are used to produce this probabilistic solution. The residential areas are shaded in grey, which changes the hue of the color scale.

The probability that completely dry tephra will exceed this critical threshold due to a Moderate eruption located at Eldfell is quite low (Figure 20, left). For fully saturated wet tephra, however, almost all the buildings on Heimaey have a greater than 5% probability of reaching this critical threshold (Figure 20, right). The critical threshold is not reached for a Moderate eruption located at Surtsey. The mass loading of tephra plus precipitation could be a significant threat to the buildings of Heimaey if an eruption occurs within the Vestmannaeyjar volcanic system sufficiently close to Heimaey. We cannot define how close to Heimaey a vent must be to pose such a threat based on the work completed within this report. Mitigation action plans, such as those implemented during the 1973 eruption, including tephra removal from buildings and insertion of support beams inside of buildings, should consider how precipitation may be adding to the total mass load and creating a threat to buildings that might be sufficiently strong if the tephra was dry.

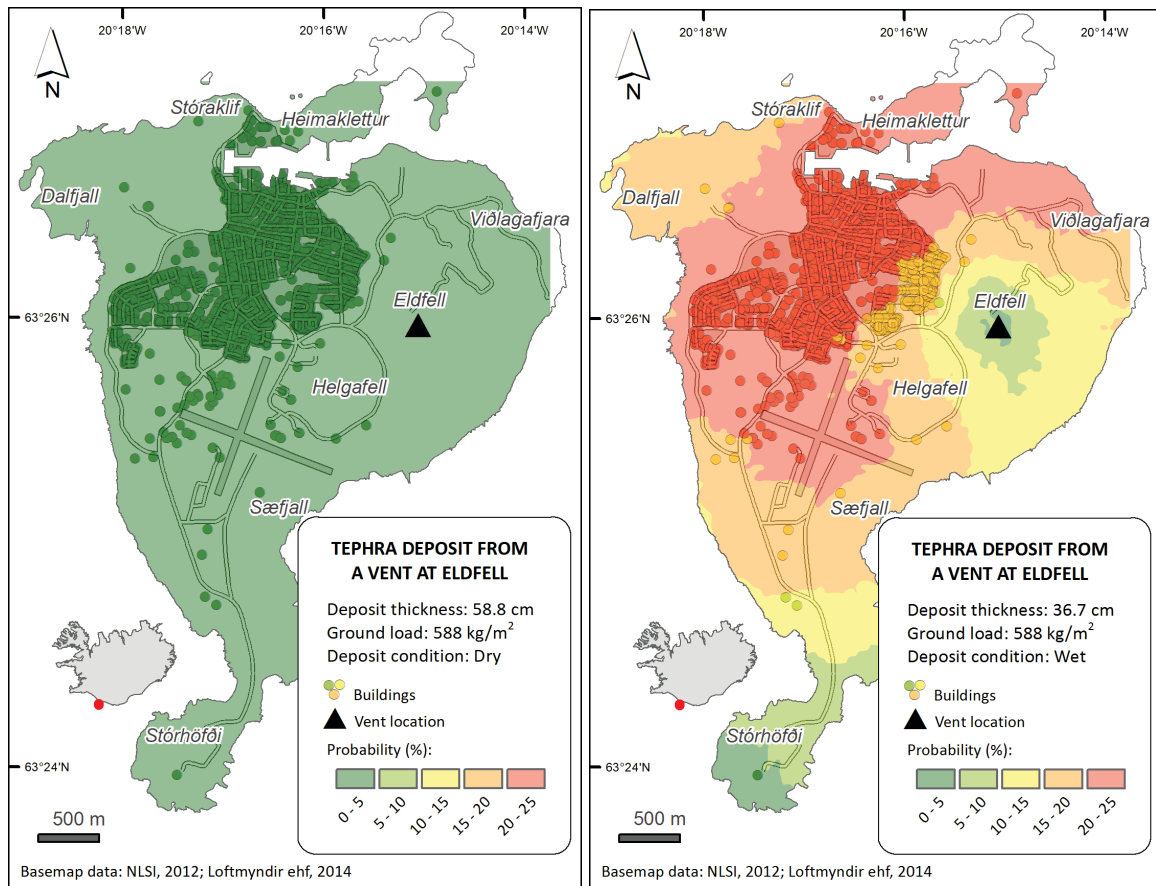


Figure 20: Exceedance probabilities for accumulation of tephra from a vent at Eldfell dry (left) and wet (fully saturated, right) released from a six-day long Moderate eruption with a load of at least 588 kg/m² (thickness of 58.8 cm or 36.7 cm, respectively). Ten years of meteorological data are used to produce this probabilistic solution. Buildings are shown as more intense, but the same color as the area they are in. The residential areas are shaded in grey, which changes the hue of the color scale.

5.3 Direct economic costs

Different modeling approaches were used for assessing the potential impact from tephra fall and lava inundation. The lava flow simulations utilized three eruption sizes and considered a multitude of vent locations on Heimaey only. The tephra simulations utilized only one eruption size and two vent locations (Eldfell and Surtsey) and considered a multitude of meteorological conditions. A Moderate eruption from a vent located at Surtsey is modeled to deposit too little tephra on the island to be a significant threat to infrastructure due to mass loading, but it may have an impact on road and airport runway resistance to skidding. A Moderate eruption from a vent located at Eldfell can have a significant economic impact on Heimaey due to mass loading on the buildings, but only if the tephra is wet. Completely dry tephra is not modeled to be sufficiently heavy to cause a threat to the buildings.

Iceland does not presently have a fixed acceptable risk threshold for hazards from volcanic eruptions e.g. for destruction of infrastructure, however this important work should be done. In order to analyze the costs of potential impacts, we have tabulated the economic costs of infrastructure destruction using discretized steps of acceptable risk for risk thresholds from 5%

to 40% at 5% intervals (Figure 21). Use of a high acceptable risk threshold results in lower economic cost because buildings in lower likelihood areas will not be included in the calculation, it is less conservative. If the acceptable risk is set to a low value, buildings with a lower likelihood of destruction will be included in the calculation, and therefore the potential economic impact will be high. For example, if there is at least a 5% probability of a residential structure receiving at least 588 kg/m² of fully saturated tephra (where 50% of residences in Heimaey could be anticipated to collapse; 50% of residences would be expected to withstand this mass loading; Appendix E) given an eruption located at the same site as the 1973 Eldfell eruption, then the structure's value is included in the sum for 5% acceptable risk. All buildings that are not residences were excluded from the calculation, as we have not collated information about the load-bearing capacity of these buildings, and these buildings are more likely to have tephra removed from their roofs during an eruption. The residential buildings form the majority (64%) of the total economic value of infrastructure on the island. In Appendix F we provide two complete tables for the 5% (Table 7) and 25% (Table 8) thresholds, to show how the economic cost to different categories of infrastructure changes due to the use of different acceptable risk thresholds. These economic calculations assume that no mitigating interventions are taken.

In the economic impact analysis we have made, lava flows are considered able to destroy all buildings within an area of lava inundation, but tephra mass loading is only considered able to destroy residential buildings. At the lowest acceptable risk values, the Moderate and Large lava flows could be the most expensive hazard. As the acceptable risk values increase, the unweighted lava flow scenario (ignoring enhanced spatial likelihood of where future vents may open) produces the highest potential economic harm. This impact on the economic assessment of neglecting the models of future vent opening preference is seen most significantly as eruption size decreases, because Small lava flows do not travel far from their vent. The Small eruption scenario is only modeled to threaten the infrastructure at greater than 5% likelihood in the unweighted scenario; for the normal distribution and Gaussian kernel-smoothed function weightings, lava inundation due to a Small eruption never threatens the infrastructure at greater than 5% likelihood.

At the 5% acceptable risk threshold, there is little difference in the threat to the residential buildings from mass loading and large lava flows. As the lava scenario decreases in size, the impact of applying a probability of future vent locations becomes apparent, as both the normal distribution and Gaussian kernel-smoothed function models decrease the modeled possible economic harm from a Moderate sized eruption, while the unweighted results show little difference between the Large and Moderate sized scenarios.

The second largest class of infrastructure are commercial buildings which are calculated to be worth 22% of the total economic value of infrastructure on the island. At the 5% acceptable risk threshold, the commercial buildings are uniformly threatened by lava inundation from Large and Moderate lava flows. Potential spatial weighting of the likelihood of future vent openings does not change these results. At the 25% acceptable risk threshold, the weighting of potential vent opening locations has a larger impact on the calculated economic harm than the size of the eruption scenario.

Economic vulnerability is greatest in the most densely populated parts of the island, particularly in the north around the harbor. At the lowest acceptable risk threshold of building destruction (5%), most residences are vulnerable to damage from the deposition of wet tephra from a Moderate eruption and lava inundation from a Large eruption (94% to almost all the infrastructure is threatened). At a higher risk threshold of building destruction (25%) the unweighted lava flows in both the Moderate and Large eruption scenarios are the greatest threat to the island's infrastructure. The airport facilities are not threatened by any of the scenarios at greater than 25% likelihood of destruction. The airport is in a less vulnerable part of the island than the most densely populated north. The hospital located at Sóhlíð 20 (seen in Table 7 as "Medical facilities") and the utilities are only vulnerable at greater than a 25% likelihood under the unweighted Large and Moderate lava flow scenarios.

6 Mitigation and preparedness

6.1 Warning and forecasting

The current state of the *early warning system* is described here. This system is continually evolving so this section is applicable as of December 2021.

6.1.1 Pre-eruption monitoring

As of November 2017, the continuous pre-eruptive monitoring of the Vestmannaeyjar volcanic system includes three seismic instruments, two in Heimaey and one in Bjarnarey. One of the seismic stations in Heimaey is in temporary operation, while a suitable place for the permanent Heimaey site is sought. There has been ongoing research to improve the seismic monitoring of the Vestmannaeyjar volcanic system via measures to improve earthquake location accuracy of events under Heimaey. It is believed that the earthquakes detected near to Heimaey are located too far west to their true location. It has been under study for more than five years to attempt and constrain this through temporary deployments of seismometers around Heimaey and on neighboring skerries. Due to the very small number of earthquakes it is still under research where seismometers can be most effectively located and how to best correct for this apparent displacement.

There is great community interest in improving the seismic monitoring of Heimaey and to advance this work. By the end of 2021 IMO will provide a work plan for improving the seismic monitoring of the island. It is essential for more earthquakes to be detected to advance this work. The very low number of earthquakes slows this progress down.

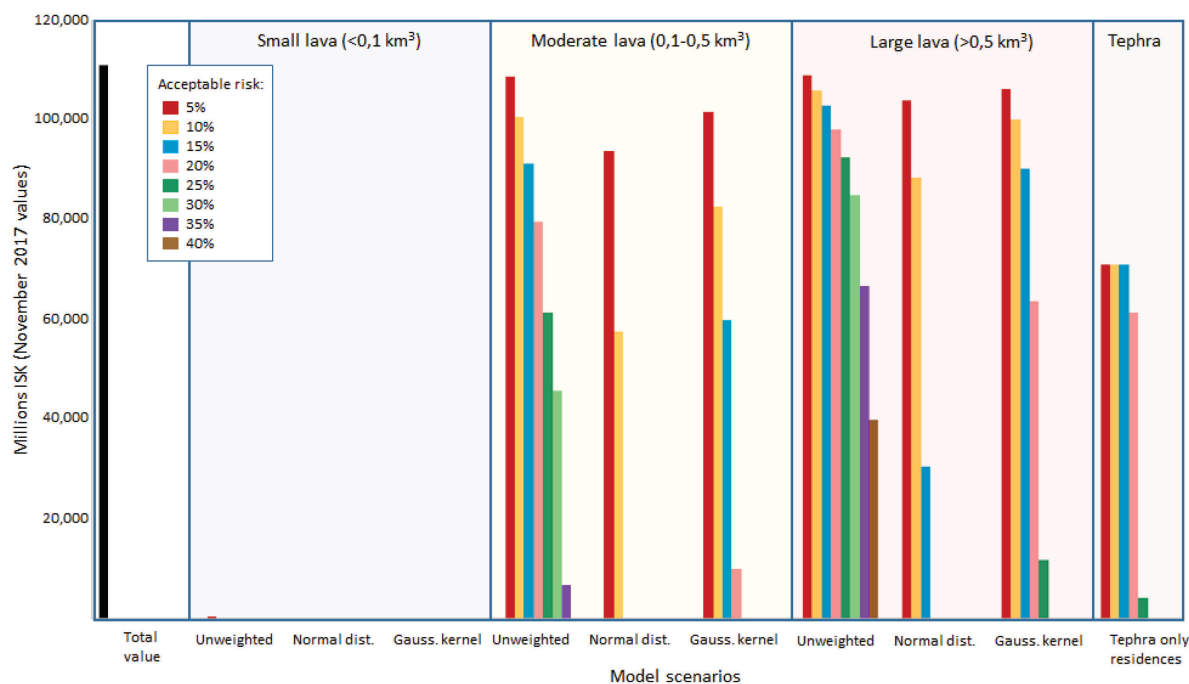


Figure 21: Direct economic cost of infrastructure destruction for the different eruption scenarios and hazards using discretized steps of acceptable risk of building destruction. The total value of infrastructure on the island is shown in black. If the acceptable risk of building destruction is low (e.g. 5%), all buildings with a low (5%) likelihood of being destroyed are included, and therefore the potential economic cost will be high. In the small eruption scenarios, the lava travels such a short distance from the vent that there is little opportunity for one geographical region to be more vulnerable than other, and therefore it only appears at the 5% acceptable risk threshold for the Unweighted scenario, but is so little value it is hard to see.

In addition to the seismic monitoring there is one continuous GPS instrument in the middle west part of Heimaey and there are regular visits to measure the composition of gases being emitted from the high-temperature regions of Eldfell and Surtsey.

Seismicity was detected prior to both the 1963 and 1973 eruptions and it is anticipated that seismic activity will be a precursory signal to future eruptions. In 1973 the activity started about 48 hours before the eruption onset. IMO currently has natural hazard specialists monitoring Iceland 24/7. The continuous data streams (on Heimaey, seismic and GPS) are followed constantly and earthquakes are automatically located within two minutes. The automatic locations are reviewed and improved when necessary within minutes to hours by the natural hazard specialist on duty. Volcano experts within and outside of IMO are available for consultation and a specific protocol is defined if the volcanic unrest advances too quickly for consultation. The level of monitoring, both with regards to instrumentation and committed human resources, are improved today compared with prior to the 1963 and 1973 eruptions.

The focus of the Civil Protection and Emergency Management is prevention, preparedness, response and recovery for natural and man-made disasters. The NCIP is responsible for civil protection and emergency management in Iceland. At the local level the Chiefs of Police and Civil Protection Committees are responsible for civil protection activities and response plans in collaboration with the NCIP-DCPEM. The prevention and preparedness actions involve risk

reduction and mitigation measures to avoid the adverse impacts of hazards and related disasters upon people, property, livelihoods and the environment. These measures aim to reduce vulnerability and exposure to disasters, and to increase resilience in disaster prone areas by strengthening the livelihoods of the inhabitants, their coping mechanism and risk knowledge. Preparedness actions aim to build the capacities needed to efficiently manage emergencies and are based on analysis of disaster risks, contingency planning, and the development of disaster management. Activities include coordination, planning, preparation of equipment, evacuation planning, education and public information strategies as well as training and exercises. All these must be supported by formal institutional, legal and budgetary capacities (Civil Protection Act No. 82/2008).

If volcanic unrest is detected, and there is sufficient time for consultation, the NCIP-DCPEM can request a meeting of the Civil Protection Scientific Advisory Board (CPSAB) which includes experts from IMO, IES, the Directorate of Health, the Environment Agency of Iceland, and others as needed. CPSAB meetings happen regularly during times of volcanic unrest, for example during the magmatic intrusions in the Reykjanes Peninsula throughout 2020 and during the 2014-2015 Holuhraun eruption.

6.1.2 Communication of risk

IMO designs and follows internal contingency plans for its activities regarding natural hazards including volcanic eruptions. The main stakeholders prior to and during volcanic eruption are the general public, civil protection, road authorities and energy companies, and aviation-related stakeholders including Isavia, the company responsible for air navigation services in the air traffic control area of Iceland, and the London Volcanic Ash Advisory Centre. IMO's contingency plan for a volcanic eruption is tested monthly, ensuring that the working procedures, communication, software and hardware are functioning properly. IMO provides information about the ongoing event to the general public via website, media and social networks, and there are people available day and night to answer questions by telephone and email. IMO communicates with NCIP-DCPEM via phone calls and regular meetings. These meetings include members of the CPSAB. At these meetings, discussion topics include possible scenarios and evolution of ongoing unrest, monitoring data, assessment of hazards, forecasts of impacts from tephra, gas, floods, etc., and scientific advice for risk mitigation actions. Factsheets and updates are created by the scientific advisory board and provided to the media and published on IMO's and NCIP-DCPEM's websites. During volcanic unrest and/or volcanic eruption IMO releases information to the aviation community via Volcano Observatory Notification for Aviation (VONA) which is sent by email to a wide, international post list of stakeholders. Significant Meteorological notices (SIGMET) are sent out when an eruption is imminent or has started and when tephra is produced during an eruption. SIGMETs are available at <http://en.vedur.is/weather/aviation/sigmet/>.

IMO is also using an Aviation Color Code system to communicate volcanic unrest available at en.vedur.is/weather/aviation/volcanic-hazards/. Color codes, which are in accordance with recommended International Civil Aviation Organization (ICAO) procedures, are intended to inform the aviation sector about a volcano's status. Notifications are issued for both increasing and decreasing volcanic activity and are accompanied by text with details (as known) about the nature of the unrest or eruption, especially tephra-plume information and descriptions of likely outcomes.

The NCIP is responsible for assigning alert levels and evacuation orders in collaboration with the relevant Chiefs of Police for all natural (except for avalanche where IMO has the responsibility) and man-made hazards. There are three alert levels: Uncertainty Phase, Alert Phase and Emergency Phase corresponding to the severity of the situation (Reglugerð um flokkun almannavarnastiga No. 650/2009). An alert level is activated based on risk assessment and scientific advice from the Civil Protection Scientific Advisory Board, information from the local authority, or other reliable information. If needed, the DCPEM sends out SMS text messages to mobile phones in the emergency area via cell broadcasting to inform the public about a hazardous event or the onset of an emergency. Risk is mainly communicated from the DCPEM website and Social Media, but also by news releases, SMS and emails radio and television. This includes information to governmental agencies, stakeholders and the public. The National Crisis and Coordination Centre (NCCC) is activated during emergencies and then the risk communication is the responsibility of the Centre. A representative from the Icelandic State Broadcasting System has a role in the NCCC to broadcast information and communicate risk. During large emergencies a Civil Protection media team is activated in the NCCC to ensure risk communication to local, national and international media with a holistic approach to disseminate information. The media team consists of media representatives from different governmental institutions and ministries.

6.2 Risk acceptance

Different communities have different perceptions of risk and levels of acceptable risk based on their lived experiences. A committee established by the Ministry of Environment and Natural Resources in 2016 is currently working to define the acceptable volcanic risk within Icelandic society. The work accomplished by this committee will likely be written into laws and regulations in the future, as has been done for avalanches. In the future, the results of this initial project together with the results of the definition of acceptable volcanic risk in Icelandic society can be used to generate a comprehensive assessment of volcanic risk to infrastructure in Iceland.

6.3 Comprehensive risk assessment

A comprehensive risk assessment combines the determined vulnerability and the societally defined risk acceptance levels. This is beyond the scope of this initial project, as the risk acceptance has not yet been defined.

6.4 Knowledge building in society

In 2011 the Civil Protection and Emergency Management in Vestmannaeyjar in collaboration with the NCIP prepared a report on hazards, risk and resilience in the Vestmannaeyjar archipelago (Jóhannesdóttir & Lögreglustjórinn í Vestmannaeyjum, 2011). One of the main concerns was a lack of research and material for the public of the Vestmannaeyjar volcanic system, especially following the two recent eruptions. One of the main outcomes from this report was statement of need for a contingency plan for future volcanic eruptions. In January 2017, a contingency plan for volcanic eruptions in Vestmannaeyjar was published after extensive work with first responders, governmental authorities and stakeholders (Lögreglustjórinn í Vestmannaeyjum, almannavarnadeild ríkislögreglustjóra & almannavarnanefnd Vestmannaeyja, 2017).

This initial hazard assessment is a step forward from the previous report in 2011 largely due to the integration of previous knowledge with modeling techniques newly applied here. The results of this report will be available to residents and visitors on the internet. The foundational knowledge used to prepare this report will be used to update the Catalogue of Icelandic Volcanoes. This technical report is written in English and is a supplement to the report in Icelandic *Forgreining á hættu vegna goss á eldstöðvakerfi Vestmannaeyja. Frummat á áhrifum hraunrennslis og öskufalls í Heimaey* (Pfeffer et al., 2021).

The 1973 volcanic eruption was unexpected for the local population with only minor precursors and only minor earthquakes were felt on the island just before the eruption (Sólnes et al., 2013). The inhabitants were unaware of the risk despite the Surtsey eruption which had ended just a few years prior. Today people are better informed about the risk of volcanic hazard and the memory of what happened is kept alive.

To commemorate the end of the eruption and ensure knowledge transfer, the islanders celebrate the Goslokahátíð (The end of the eruption festival). The celebration lasts for four days in the beginning of July. The celebration includes activities such as planting trees, attending exhibitions, hikes, music festivals and children's activities. In the town of Vestmannaeyjar there is a very informative and popular museum, Eldheimar, that reminds the locals and informs visitors of the eruption that changed the life of an entire community.

6.5 Evacuation response plans

The contingency plan for a volcanic eruption in the Vestmannaeyjar volcanic system is available in Icelandic at www.almannavarnir.is/utgefid-efni/vidbragdsaaetlun-vegna-eldgossi-vestmannaeyjum-utgafa-1-0-23-01-2017/?wpdmdl=22104 (Lögreglustjórinn í Vestmannaeyjum et al., 2017).

The contingency plan for a volcanic eruption in the Vestmannaeyjar region deals with the command and control within the emergency management system during volcanic unrest. The same system is in place if there is an evacuation order. The aim is to ensure an organized response to a volcanic eruption in the Vestmannaeyjar region and assist the population in the best possible manner. The National Commissioner of the Icelandic Police in collaboration with the Commissioner of Police in Vestmannaeyjar is responsible for the activation of the plan which must be updated at least every four years. The plan must be exercised regularly. In the region of Vestmannaeyjar there is one police station situated on Heimaey. There is a rescue team on the island, Björgunarfélag Vestmannaeyja, with 30 volunteers. In Iceland there is a network of about 100 Icelandic Search and Rescue (ICE-SAR) teams and there are always thousands of volunteers available for rescue work from the mainland. The rescue teams have extensive experience, training and knowledge in rescue operations in various conditions both at sea and on land. The Red Cross oversees emergency shelter during disasters. The emergency shelters provide disaster victims with safe facilities where they can eat and rest as well as seek counselling and psychosocial support. The Icelandic Civil Protection has a special contract with the rescue teams and the Red Cross to assist during disasters. During recent volcanic eruptions both the Red Cross and ICE-SAR played an important role.

In 1963, likely following the onset of the Surtsey eruption, there was made an estimate of the capacity of the fishing vessels to aid with evacuation in case of an eruption on Heimaey. The goal was to be able to move everyone to safety in case of an eruption. This plan was never completed, however its goals were accomplished in 1973 when almost all the >5.000 inhabitants were evacuated. At the onset of the eruption the fishing fleet was in the harbor and

thus available to assist with the evacuation. Around 60 fishing vessels were used to evacuate the inhabitants and some of their belongings to the mainland in a matter of hours.

The structure and general plan of the Civil Protection System in Iceland had only just been developed and in 1972 the first emergency plans for an eruption in Katla volcano and two other municipalities had been made. The general plan that was used during the evacuation in Heimaey emphasized the need for localized plans during emergencies. This is now a standard procedure and in addition to the general plan there are also localized plans for specific risks in specific places in Iceland. Lessons that can be drawn from the eruption in 1973 show that risk reduction and mitigation measures must be an ongoing process. During the eruption, all the island's critical infrastructure was impacted, including buildings, roads, power, water and the fishing industry.

The inhabitants and hundreds of volunteers rescuing valuables were exposed to poisonous gases, tephra, lava flow and lava bombs. The harbor, the lifeline of the island, was initially threatened by the lava flow. Efforts to divert the advancing lava flow away from the harbor by spraying seawater onto the lava flow were successful and at the last minute the harbor was saved.

Many of the inhabitants returned to build back what had been destroyed during the eruption. Consequences from the eruption included loss of livelihood and displacement from the homes where many of the residents had lived all their lives. Psychosocial support that was not available at the time of the eruption is recognized today as an important part of a recovery process. Today there is a National system of psychosocial support in Iceland and there is a division in Vestmannaeyjar that supports the inhabitants when they need assistance.

6.6 Mitigation

Mitigation actions related to the volcanic hazards of tephra fall and lava inundation could include: engineering and construction of robust infrastructure, constructing infrastructure in areas that are less vulnerable to the hazards, removing tephra from building and roads, reinforcing ceilings, attempting to redirect lava, as well as education and raising awareness within the local community. The choice of when and how to deploy mitigation actions is dependent on the definition of acceptable risk and the laws and regulations that follow from that. Results from initial risk assessment work, like this, can be used to provide suggestions regarding more/less advisable locations for infrastructure. Heimaey's political bodies will decide how to utilize these suggestions, or to request further analysis of the project's results that could benefit their planning.

7 Conclusions and Recommendations

7.1 Conclusions

Eruption frequency for the Vestmannaeyjar volcanic system is understood to be low relative to the more active volcanoes of the EVZ. Moreover, this study indicates that there is a low, 3–8% likelihood that the next eruptive vent will open on Heimaey/92–97% likelihood that the next eruptive vent will not open on Heimaey. This is, however, an underestimation if future activity is more likely to occur around Heimaey.

The analysis presented here is intended to be an initial step of a comprehensive long-term assessment of volcanic hazards that can be developed as we gain more thorough understanding of the geological background of the volcanic system.

This study simulates the potential effects of three sizes of lava flows on Heimaey and one size of tephra fall from Eldfell and Surtsey on critical infrastructure. Effects from lava flow inundation were calculated based on three models of future vent location likelihood: 1) unweighted (all modeled vents on Heimaey being equally likely); 2) normal distribution around a best fit line of previous vents; and 3) a Gaussian kernel-smoothed function of previous vents. None of these models use the ages of the identified eruption vents in the calculation.

As the volume of lava increases (eruption size increases) greater differences in regional vulnerability for lava inundation at different parts of the island are seen. The potential damage from lava inundation from a Small eruption is locally restricted and regional differences in vulnerability to Small lava flows are minor.

The most densely populated parts of Heimaey in the north and around the harbor are the most vulnerable, and the southern and eastern parts of the island are least vulnerable, to Moderate and Large lava flows originating on the island. Almost all infrastructure is vulnerable to lava inundation from a Large eruption anywhere on the island at a 5% likelihood of the building being inundated.

Most of the roads in Heimaey and the airport runways have a greater than 5% probability of tephra deposits being within the critical range of 1–5 mm that can reduce resistance to skidding if an eruption vent is located at Eldfell or Surtsey. This suggests that the potential for hazardous tephra deposits on roads and airport runways on Heimaey should be considered for all eruptions of the Vestmannaeyjar system regardless of vent location, and potentially from other Icelandic volcanoes as well.

Heimaey residence roofs were analyzed with regards to ability to withstand mass loading. Half (fifty percent) of the Heimaey residence roofs are vulnerable to collapse at 588 kg/m² mass loading. This mass is modeled to be reached within six days of some Moderate sized eruptions if the eruption occurs on Heimaey (near), if the winds promote transport over the island and if the tephra is wet (precipitation increases mass). This mass loading is not modeled to be reached within six days if the vent is at Surtsey (far), if the winds blow the tephra away from the island, or if the tephra is dry.

There is a 15% likelihood that almost all residences will be exposed to tephra mass loading higher than the critical mass load for wet tephra from a Moderate eruption from Eldfell.

The most densely populated areas in the northern parts of the island are the most vulnerable parts of Heimaey to tephra mass loading from an eruption at Eldfell.

Higher thresholds for acceptable risk imply that the threshold is less likely to be met. The Small lava flow scenario only has a significant economic cost at a 5% acceptable risk threshold, the lowest, most conservative, and easiest to reach threshold analyzed. At the highest threshold analyzed in this report, 40%, only the Large lava flow scenario without vent location weighting shows an economic cost. The models for regional likelihood of vent opening have large impacts on the calculated economic cost.

All the cost calculations do not consider mitigation actions, such as clearing tephra from roofs and roads, reinforcing ceilings, and redirecting lava. Mitigation actions have proved to be very beneficial during the 1973 eruption and the experiences from this eruption should be relied on to help guide future actions.

In the event of volcanic unrest, the 24/7 natural hazards specialist on duty at IMO has experts within and outside of IMO to confer with as well as a specific protocol to follow if the volcanic unrest advances too quickly for consultation. Notifications are issued for both increasing and decreasing volcanic activity and are accompanied by details about the nature of the unrest or eruption.

The number of people on Heimaey varies significantly depending on time of day, season and if it is a special event. Many Icelandic and foreign visitors come to the island. Contingency plans need to take this extremely large range of possibly vulnerable people into consideration. There can be additionally huge numbers of visitors on special occasions which will impact evacuations during the summer months. The best case for evacuations would be that they are completed before the onset of an eruption or shortly thereafter.

7.2 Recommendations

This preliminary risk assessment only focused on lava flow and tephra fall from selected scenarios. Some other important hazards, including gases and flammable ballistics, are not included in this work due to insufficient foundational information, although the only fatality in the 1973 eruption was from gas exposure. We recommend that evaluation of these hazards should be included in future volcanic risk and hazard assessment projects when possible.

More research is needed on the ages of the identifiable vents in order to revisit the models for future vent location probability and to further study the temporal likelihood of future eruptions of the Vestmannaeyjar system.

In this work we treat the eruptions as single vents. In future work, the possibility of fissure eruptions should be considered, as well.

Additional analysis is needed on the mass loading capacity loading capacity of buildings other than residences, such as schools and other critical buildings.

The cascading economic and social impacts of damage to community infrastructure should be considered in detail in later studies.

Where settlements have been built close to volcanically active areas it is essential that communities and governing authorities understand the nature of volcanic hazards and make plans for mitigating the associated risk. In the case of Vestmannaeyjar, pre-eruption mitigation can occur in a variety of ways, ranging from building up knowledge on the emergency responses in the unlikely event of an eruption, to risk reduction using land-use planning. Future developments could thus consider increasing the geographical distribution of new buildings and facilities, so the critical infrastructure is less concentrated in the most vulnerable locations.

Real-time monitoring of pre-eruptive indicators such as seismicity, deformation and gas emissions their incorporation into eruption forecasts play an important role in volcanic risk mitigation and those monitoring systems should be maintained. In particular the seismic monitoring should be improved by identifying optimal seismic station locations and updating the earthquake location algorithms.

Numerical simulations of the time-dependent spread of lava should be made for specific examples. These results could be used to further improve mitigation and evacuation plans by identifying the possible timing and extent of lava hazards to constrain the time available for evacuation, in addition to analyzing potential evacuation routes.

Work on defining acceptable volcanic risk in Iceland is currently being undertaken as a basis for future legislation and policy. When this threshold has been defined, this report should be revisited with these specific definitions in mind.

8 Acknowledgments

We would like to thank the advisory committee for the project. We would also like to thank Kristján Sæmundsson, Trausti Jónsson, Verkís, Sigurlaug Gunnlaugsdóttir, Haraldur Sigurðsson, Heather Wright, the Civil Defense Commission of Vestmannaeyjar and Víðir Reynisson.

References

- Barsotti, S., Neri, A. & Scire, J.S. (2008). The VOL-CALPUFF model for atmospheric ash dispersal: 1. Approach and physical formulation. *Journal of Geophysical Research*, 113(B3). doi:10.1029/2006JB004623
- Barsotti, S., Di Rienzo, D.I., Thordarson, T., Björnsson, B.B. & Karlsdóttir, S. (2018). Assessing Impact to Infrastructures Due to Tephra Fallout From Öræfajökull Volcano (Iceland) by Using a Scenario-Based Approach and a Numerical Model. *Frontiers in Earth Science*, 6. doi.org/10.3389/feart.2018.00196
- Barsotti, S., S. Karlsdóttir, A.M. Ágústsdóttir, B. Oddsson, Í. Marelldóttir, Þ. Þórðarson, Þ. Guðnason & B.B. Björnsson (2020). *Preliminary tephra fallout hazard assessment for selected eruptive scenarios in Iceland*. Report published by the Icelandic Meteorological Office VÍ 2020-004. www.vedur.is/media/vedurstofan-utgafa-2020/VI_2020_004.pdf
- Biass, S. & Bonadonna, C. (2014). *TOTGS: Total grainsize distribution of tephra fallout*. Retrieved from <https://vhub.org/resources/3297>
- Blackburn, E.A., Wilson, L. & Sparks, R.S.J. (1976). Mechanisms and dynamics of strombolian activity. *Journal of the Geological Society*, 132(4), 429–440. doi:10.1144/gsjgs.132.4.0429
- Blake, D., Wilson, T., Cole, J., Deligne, N. & Lindsay, J. (2017). Impact of Volcanic Ash on Road and Airfield Surface Skid Resistance. *Sustainability*, 9(8), 1389. doi:10.3390/su9081389
- Bobrowsky, P.T. (ed.). (2013). *Encyclopedia of natural hazards*. Dordrecht; New York: Springer
- Bonadonna, C. & Houghton, B.F. (2005). Total grain-size distribution and volume of tephra-fall deposits. *Bulletin of Volcanology*, 67(5), 441–456. doi:10.1007/s00445-004-0386-2
- Burton, R.R., Dudhia, J., Gadian, A.M. & Mobbs, S.D. (2017). The use of a numerical weather prediction model to simulate the release of a dense gas with an application to the Lake Nyos disaster of 1986: Simulating the release of a dense gas. *Meteorological Applications*, 24(1), 43–51. doi:10.1002/met.1603
- Catalogue of Icelandic Volcanoes. <http://icelandicvolcanoes.is>
- Civil Protection Act No. 82/2008. www.government.is/publications/legislation/lex/2017/12/21/Civil-Protection-Act-No.-82-2008
- Egilson, D. (1974). *Athuganir á gjallfalli í Heimeyjargosi 1973*. University of Iceland, Reykjavík
- Guðmundsson, M.T., Larsen, G., Höskuldsson, Á. & Gylfason, Á.G. (2008). Volcanic hazards in Iceland. *Jökull*, (58), 251–268
- Guðmundsson, R. (2016). *Ferðamenn og íbúar í Vestmannaeyjum 2016*. Vestmannaeyjabær: Rannsóknir og ráðgjöf ferðaþjónustunnar ehf
- Guðmundsson, R. (2018). *Ferðamenn í Vestmannaeyjum 2004–2018*. (Samantekt unnin fyrir Þekkingarsetur Vestmannaeyja). Hafnarfjörður: Rannsóknir og ráðgjöf ferðaþjónustunnar ehf. 10 bls.
- Guffanti, M., Mayberry, G.C., Casadevall, T.J. & Wunderman, R. (2009). Volcanic hazards to airports. *Natural Hazards*, 51(2), 287–302. doi:10.1007/s11069-008-9254-2
- Höskuldsson, Á. (2015). Vestmannaeyjar. Alternative name: Eyjar. In Ilyinskaya, E., Larsen, G., & Guðmundsson, M.T. (eds.): *Catalogue of Icelandic Volcanoes*. IMO, UI, CPD-NCIP. Retrieved from <http://icelandicvolcanoes.is/?volcano=VES>
- Höskuldsson, Á., Hey, R., Vésteinsson, Á.Þ. & Kjartansson, E. (February 21, 2009). *Volcanism in the Vestmannaeyjar volcanic system during the past 20 ka*. Poster flutt á Marine Research Institute Conference, Reykjavík. Retrieved on October 19, 2017 from www.hafro.is/hafradstefna/fyrirlestrar_posters/armann.vestmannaeyjar.poster.pdf

- Höskuldsson, Á., Kjartansson, E., Vésteinsson, Á.Þ., Steinþórsson, S. & Sigurðsson, O. (2013). Eldstöðvar í sjó. In Sólnes, J., Sigmundsson, F. and Bessason, B. (eds.) *Náttúruvá á Íslandi – Eldgos og jarðskjálftar*. Reykjavík: Háskólaútgáfan
- Iceland GeoSurvey. (2008). 25-meter Digital Elevation Model of Iceland. Dataset
- Icelandic Coast Guard Hydrographic Department & University of Iceland Institute of Earth Sciences. (2007). Multibeam survey. Dataset
- Icelandic Standards. IST120:2012. Retrieved from www.stadlar.is/stadlabudin/vara/?ProductName=IST-120-2012
- Jakobsson, S.P. (1968). The geology and petrography of the Vestmann Islands: A preliminary report. *Surtsey Research Progress Report, IV*, 113–129
- Jakobsson, S.P. (1975). Jarðfræðikort (Heimaey, Vestmannaeyjum). Bæjarsjóður Vestmannaeyja
- Jakobsson, S.P. (1979). Petrology of Recent Basalts of the Eastern Volcanic Zone, Iceland. *Acta Naturalia Islandica*, 26, 109 p.
- Jakobsson, S.P., Pedersen, A.K., Rönso, J.G. & Melchior Larsen, L. (1973). Petrology of mugearite-hawaiite: Early extrusives in the 1973 Heimaey eruption, Iceland. *Lithos*, 6(2), 203–214. doi:10.1016/0024-4937(73)90065-0
- Jamtveit, B., Brooker, R., Brooks, K., Larsen, L.M. & Pedersen, T. (2001). The water content of olivines from the North Atlantic Volcanic Province. *Earth and Planetary Science Letters*, 186(3–4), 401–415. doi:10.1016/S0012-821X(01)00256-4
- Jóhannesdóttir, G. & Lögreglustjórinn í Vestmannaeyjum (2011). *Áhættusköðun almannavarna í umdæmi lögreglustjórans í Vestmannaeyjum*. Vestmannaeyjabær. Retrieved 1. February 2018 from www.almannavarnir.is/utgefing-efni/ahaettuskodun-almannavarna-i-umdaemi-logreglustjorans-i-vestmannaeyjum/?wpdmml=21529
- Jóhannesson, H. (1983). Eldgos við Vestmannaeyjar 1637–38. *Náttúrufræðingurinn*, 52, 33–36
- Jóhannesson, H. & Sæmundsson, K. (1998). Geological map of Iceland, 1:500,000, Bedrock geology. Reykjavík: Icelandic Institute of Natural History
- Jóhannesson, T. (2017). Risk management in avalanche-prone areas in Iceland (revised). *Visionen im Lawinenschutz / Avalanche Protection - Visions*, 179, 86–97
- Kjartansson, G. (1966). Nokkrar nýjar C14-aldursákvarðanir. *Náttúrufræðingurinn*, 36(3), 126–141
- LBCS. Land-Based Classification Standards. Retrieved from www.planning.org/lbcs/standards/structure
- Loftmyndir ehf. (2014). 2-meter Digital Elevation Model of Heimaey. Dataset
- Lögreglustjórinn í Vestmannaeyjum, almannavarnadeild ríkislögreglustjóra & almannavarnanefnd Vestmannaeyja. (2017). *Viðbragðsáætlun vegna eldgoss í Vestmannaeyjum*. Retrieved on February 1, 2018 from www.almannavarnir.is/utgefing-efni/vidbragdsaaetlun-vegna-eldgoss-i-vestmannaeyjum-utgafa-1-0-23-01-2017/?wpdmml=22104
- Martin, A.J., Umeda, K., Connor, C.B., Weller, J.N., Zhao, D. & Takahashi, M. (2004). Modeling long-term volcanic hazards through Bayesian inference: An example from the Tohoku volcanic arc, Japan: Bayesian inference of volcanism. *Journal of Geophysical Research: Solid Earth*, 109(B10). doi:10.1029/2004JB003201
- Mattsson, H. & Höskuldsson, Á. (2003). Geology of the Heimaey volcanic centre, south Iceland: early evolution of a central volcano in a propagating rift? *Journal of Volcanology and Geothermal Research*, 127(1–2), 55–71. doi:10.1016/S0377-0273(03)00178-1
- Mattsson, H.B. & Höskuldsson, Á. (2005). Eruption reconstruction, formation of flow-lobe tumuli and eruption duration in the 5900 BP Helgafell lava field (Heimaey), south Iceland. *Journal of Volcanology and Geothermal Research*, 147(1–2), 157–172. doi:10.1016/j.jvolgeores.2005.04.001

- Meyer, P.S., Sigurdsson, H. & Schilling, J. (1985). Petrological and geochemical variations along Iceland's Neovolcanic Zones. *Journal of Geophysical Research*, 90(B12), 10043. doi:10.1029/JB090iB12p10043
- Michieli Vitturi, M. de' & Tarquini, S. (2018). MrLavaLoba: A new probabilistic model for the simulation of lava flows as a settling process. *Journal of Volcanology and Geothermal Research*. doi:10.1016/j.jvolgeores.2017.11.016
- Mitchell, N.C., Beier, C., Rosin, P.L., Quartau, R. & Tempera, F. (2008). Lava penetrating water: Submarine lava flows around the coasts of Pico Island, Azores: MORPHOLOGIES OF LAVA PENETRATING WATER. *Geochemistry, Geophysics, Geosystems*, 9(3), n/a-n/a. doi:10.1029/2007GC001725
- National Land Survey of Iceland. (2012). IS 50V version 3.4. Database
- Newhall, C. & Hoblitt, R. (2002). Constructing event trees for volcanic crises. *Bulletin of Volcanology*, 64(1), 3–20. doi:10.1007/s004450100173
- Nichols, A. R. L., Carroll, M. R. & Höskuldsson, Á. (2002). Is the Iceland hot spot also wet? Evidence from the water contents of undegassed submarine and subglacial pillow basalts. *Earth and Planetary Science Letters*, 202(1), 77–87. doi:10.1016/S0012-821X(02)00758-6
- Pagneux, E. (2015). Öraefi district and Markarfljót outwash plain: Spatio-temporal patterns in population exposure to volcanogenic floods. In E. Pagneux, M. T. Gudmundsson, S. Karlsdóttir, & M. J. Roberts (Eds.), *Volcanogenic floods in Iceland: An assessment of hazards and risks at Öraefajökull and on the Markarfljót outwash plain* (pp. 123–140). Reykjavík: IMO, IES-UI, NCIP-DCPEM
- Pagneux, E., Gudmundsson, M.T., Karlsdóttir, S. & Roberts, M.J. (2015). *Volcanogenic floods in Iceland: An assessment of hazards and risks at Öraefajökull and on the Markarfljót outwash plain*. Reykjavík: IMO, IES-UI, NCIP-DCPEM. Retrieved from www.vedur.is/gogn/vefgogn/jokulhlaup/haettumat/oraefajokull_markarfljotsaurar/bok_en/fulltext_web.pdf
- Pedersen, G.B. M., Höskuldsson, Á., Dürig, T., Thordarson, T., Jónsdóttir, I., Riishuus, M.S., ... Schmith, J. (2017). Lava field evolution and emplacement dynamics of the 2014–2015 basaltic fissure eruption at Holuhraun, Iceland. *Journal of Volcanology and Geothermal Research*, 340, 155–169. doi:10.1016/j.jvolgeores.2017.02.027
- Pfeffer, M.A., Sara Barsotti, Bergrún Óladóttir, Esther Hlíðar Jensen, Emmanuel Pierre Pagneux, Bogi Brynjar Björnsson ... Kristín S. Vogfjörð (2021). *Forgreining á hættu vegna goss á eldstöðvakerfi Vestmannaeyja. Frummat á áhrifum hraunrennslis og öskufalls*. Report published by the Icelandic Meteorological Office VÍ 2021-003. Retrieved from www.vedur.is/media/vedurstofan-utgafa-2021/VI_2021_003.pdf
- Reglugerð um flokkun almannavarnastiga No. 650/2009
- Rouwet, D., Constantinescu, R. & Sandri, L. (2017). Deterministic versus probabilistic volcano monitoring: Not "or" but "and". In Gottsmann, J., Neuberg, J., Scheu, B. (Eds). *Volcanic Unrest: From Science to Society*. Cham: Springer International Publishing, 35–46
- Self, S., Sparks, R.S.J., Booth, B. & Walker, G.P.L. (1974). The 1973 Heimaey Strombolian Scoria deposit, Iceland. *Geological Magazine*, 111(06), 539. doi:10.1017/S0016756800041583
- Selva, J., Orsi, G., Di Vito, M. A., Marzocchi, W. & Sandri, L. (2012). Probability hazard map for future vent opening at the Campi Flegrei caldera, Italy. *Bulletin of Volcanology*, 74(2), 497–510. doi:10.1007/s00445-011-0528-2
- Sigmarrsson, O. (1996). Short magma chamber residence time at an Icelandic volcano inferred from U-series disequilibria. *Nature*, 382, 440–442
- Sigurdsson, F. H. (1973). *Global Volcanism Program Bulletin Report*. Smithsonian Institution. Retrieved on June 12, 2017 from http://volcano.si.edu/volcano.cfm?vn=372010#bgvn_197301
- Sigurðsson, I.A. & Jakobsson, S.P. (2009). Jarðsaga Vestmannaeyja. In *Vestmannaeyjar*. Retrieved from https://nattsud.is/skrar/file/Jardsaga_Vestmannaeyja_heimildir.pdf

- Sigurðsson, Ó.J. (1973). *Dagbækur Óskars J. Sigurðssonar (Diary)*. Stórhöfði: Veðurstofa Íslands (unpublished)
- Sigurðsson, Þ. (1965). Some geophysical measurements and observations in Surtsey 1963–1964. *Surtsey Research Progress Report, 1*, 63–67
- Sólnes, J., Sigmundsson, F. & Bessason, B. (Eds.) (2013). *Náttúruvá á Íslandi: eldgos og jarðskjálftar*. Reykjavík: Viðlagatrygging Íslands/Háskólaútgáfan
- Spence, R. J. S., Kelman, I., Baxter, P. J., Zuccaro, G. & Petrazzuoli, S. (2005). Residential building and occupant vulnerability to tephra fall. *Natural Hazards and Earth System Science, 5*, 477–494. doi:SRef-ID: 1684-9981/nhess/2005-5-477
- Spinetti, C., Barsotti, S., Neri, A., Buongiorno, M.F., Doumaz, F. & Nannipieri, L. (2013). Investigation of the complex dynamics and structure of the 2010 Eyjafjallajökull volcanic ash cloud using multispectral images and numerical simulations: 2010 Eyjafjallajökull volcanic ash cloud. *Journal of Geophysical Research: Atmospheres, 118*(10), 4729–4747. doi:10.1002/jgrd.50328
- Sæmundson, K. (1974). Evolution of the axial rifting zone in northern Iceland and the Tjörnes Fracture Zone. *GSA Bulletin, 85*(4), 495–504
- Tarquini, S., Michieli Vitturi, M. de', Jensen, E., Pedersen, G., Barsotti, S., Coppola, D. & Pfeffer, M. (2018). Modeling lava flow propagation over a flat landscape by using MrLavaLoba: the case of the 2014–2015 eruption at Holuhraun, Iceland. *Annals of Geophysics, 61* (Vol 61). doi:10.4401/ag-7812
- Thorarinsson, S. (1973). *Global Volcanism Program Bulletin Report*. Smithsonian Institution. Retrieved on June 12, 2017 from http://volcano.si.edu/volcano.cfm?vn=372010#bgvn_197301
- Thorarinsson, S., Steinthórsson, S., Einarsson, Th., Kristmannsdóttir, H. & Oskarsson, N. (1973). The Eruption on Heimaey, Iceland. *Nature, 241*(5389), 372–375. doi:10.1038/241372a0
- Thordarson, T. (2000). Physical volcanology of lava flows on Surtsey, Iceland: A preliminary report, *11*, 109–126
- Thordarson, T. & Larsen, G. (2007). Volcanism in Iceland in historical time: Volcano types, eruption styles and eruptive history. *Journal of Geodynamics, 43*(1), 118–152. doi:10.1016/j.jog.2006.09.005
- Tonini, R., Sandri, L., Costa, A. & Selva, J. (2015). Brief Communication: The effect of submerged vents on probabilistic hazard assessment for tephra fallout. *Natural Hazards and Earth System Science, 15*(3), 409–415. doi:10.5194/nhess-15-409-2015
- UNDRR (2009). UNISDR terminology on disaster risk reduction. Retrieved from: www.undrr.org/publication/2009-unisdr-terminology-disaster-risk-reduction
- Vink, G.E. (1984). A hotspot model for Iceland and the Vøring Plateau, *Journal of Geophysical Research, 89*(B12), 9949–9959, doi:10.1029/JB089iB12p09949
- White R.S., Brown, J.W. & Smallwood, J.R. (1995). The temperature of the Iceland Mantle plume and the origin of outward-propagating V-shaped ridges. *Journal of Geological Society 152*, 1039–1045. doi.org/10.1144/GSL.JGS.1995.152.01.26
- Williams, R.S. & Moore, J.G. (1976). *Man Against Volcano: The Eruption on Heimaey, Vestmannaeyjar, Iceland* (2nd print). U.S. Geological Survey. Retrieved on October 25, 2017 from <https://pubs.usgs.gov/gip/heimaey/heimaey.pdf>
- Wolfe, C. J., Th. Bjarnason, I., VanDecar, J. C. & Solomon, S. C. (1997). Seismic structure of the Iceland mantle plume. *Nature, 385*(6613), 245–247. doi:10.1038/385245a0
- Wolff, J.A. & Sumner, J.M. (2000). Lava Fountains and Their Products. In Sigurdsson, H., Houghton, B.F., McNutt, S.R., Rymer, H., Stix, J. (Eds). *Encyclopedia of Volcanoes*. San Diego: Academic Press, 321–329
- Þjóðskrá Íslands. www.skra.is
- Þórarinnsson, S. (1965). Neðansjávargos við Ísland. *Náttúrufræðingurinn, 35*, 49–74

Appendices

A. DEM, Bathymetry, and Topography

A digital elevation model (DEM) of the Heimaey land surface was created from 1 m contour lines made in 2014 by Loftmyndir ehf. The original data were made from aerial photos taken 1 August 2014, at a flight height of 1.556 m. The data that was used to create the contour lines is point data with more than 0.5 m accuracy. The lines were converted to points and then to terrain in ArcGIS. A raster dataset was created from the terrain using 2 x 2 m pixel size. Additional land surfaces were provided by Iceland GeoSurvey (2008).

A bathymetric survey of Vestmannaeyjar and surroundings was carried out by the M/S Baldur of the Icelandic Coast Guard (Icelandic Coast Guard Hydrographic Department and University of Iceland Institute of Earth Sciences, 2007). A multibeam survey was made in two steps, in 2006 and 2007, using a Reson 8101 multibeam instrument. All data were processed with Caris software and transferred over to ArcInfo. A DEM of the sea-bed surface was created using a LIDAR Data Exchange File (LAS) dataset. The land surface and sea-bed models were then combined into one 2 x 2 m raster DEM. There is data missing between the coast and the shallow sea, where the data is interpolated, and the true surface is missing. This will create greater uncertainty when lava flows from land into the sea.

Sea-bed bathymetry data were analyzed to determine the location and binned ages of currently submarine vents. The current topography of the land above the sea and the features on the sea floor contains 47 currently identifiable vents, or places where eruptions originated from (Figure 2). We identified the 47 vents based on their shape and symmetry and height relative to their surroundings and erosional features. The vents were put into age bins based on properties observable from the bathymetry and topography data including: the presence of materials that are only erupted above sea level (tuff, scoria, hyaloclastite, lava); the presence of erosional features characteristic of interaction with waves or glaciers; and an absence of erosion indicating enough time above sea level for tuff to consolidate. These observable features were used together with geomorphological knowledge of sea level and glacial changes over the last 16,000 years (Höskuldsson et al., 2009). Additional vents may have been covered by younger deposits, eroded, outside of the mapped area, and/or incorrectly identified by us as not a vent, so this number of identified vents is our best attempt, but has a high degree of uncertainty.

The development of the unified topographic and bathymetric map allowed us to calculate a more precise volume of lava erupted during the 1973 Eldfell eruption to be 0.27 km³ (0.24 km³ DRE) This volume was calculated by examining the pre-eruptive DEM, the post-eruptive DEM, and the bathymetry data (Figure 2). Previous estimates were 0.13 km³ (0.12 km³ DRE) (Jakobsson et al., 1973) and 0.23 km³ (0.21 km³ DRE) (Mattsson & Höskuldsson, 2003). This highlights the great amount of uncertainty associated with estimates of lava volume.

B. Input parameters used to run the MrLavaLoba simulations

```
# name of the run (used to save the parameters and the output). This changes for the small, moderate,
and large scenarios.
run_name = 'center_small'
# File name of ASCII digital elevation model
source = "../DEM/land_sjor_ve10.asc"

# This flag select how multiple initial coordinates are treated:
# vent_flag = 0 => the initial lobes are on the vents coordinates
#     and the flows start initially from the first vent,
#     then from the second and so on.
# vent_flag = 1 => the initial lobes are chosen randomly from the vents
#     coordinates and each vent has the same probability
# vent_flag = 2 => the initial lobes are on the polyline connecting
#     the vents and all the point of the polyline
#     have the same probability
# vent_flag = 3 => the initial lobes are on the polyline connecting
#     the vents and all the segments of the polyline
#     have the same probability

vent_flag = 1

#Vent location. This changes each run.
x_vent = [ 4.371324019000000e+05 ]
y_vent = [ 3.279383417000000e+05 ]

# If this flag is set to 1 then a raster map is saved where the values
# represent the probability of a cell to be covered.
hazard_flag = 1

# Fraction of the volume emplaced or the area invaded (according to the flag
# flag_threshold) used to save the run_name_*_masked.asc files.
# In this way we cut the "tails" with a low thickness (*_thickness_masked.asc)
# and a low probability (*_hazard_masked.asc). The file is used also
# to check the convergence of the solutions increasing the number of flows.
# The full outputs are saved in the files run_name_*_full.asc
# The masked files are saved only when masking_threshold < 1.
masking_threshold = 0.96

# Number of flows
n_flows = 700
# Minimum number of lobes generated for each flow
min_n_lobes = 1200

# Maximum number of lobes generated for each flow
max_n_lobes = min_n_lobes

# If volume flag = 1 then the total volume is read in input, and the
# thickness or the area of the lobes are evaluated according to the
```

```

# flag fixed_dimension_flag and the relationship  $V = n \cdot \text{area} \cdot T$ .
# Otherwise the thickness and the area are read in input and the total
# volume is evaluated ( $V = n \cdot \text{area} \cdot T$ ).
volume_flag = 1

# Total volume (this value is used only when volume_flag = 1) set "1" to be confirmed.
total_volume = 10000000 # m^3 Small scenario
total_volume = 130000000 # m^3 Moderate scenario
total_volume = 650000000 # m^3 Large scenario

# This flag select which dimension of the lobe is fixed when volume_flag=1:
# fixed_dimension_flag = 1 => the area of the lobes is assigned
# fixed_dimension_flag = 2 => the thickness of the lobes is assigned
fixed_dimension_flag = 2

# Area of each lobe ( only effective when volume_flag = 0 or fixed_dimension_flag = 1 )
lobe_area = 900 # m^2

# Thickness of each lobe ( only effective when volume_flag = 0 or fixed_dimension_flag 2 )
avg_lobe_thickness = 0.05 #m

# Ratio between the thickness of the first lobe of the flow and the thickness of the
# last lobe.
# thickness_ratio < 1 => the thickness increases with lobe "age"
# thickness_ratio = 1 => all the lobes have the same thickness
# thickness_ratio > 1 => the thickness decreases with lobe "age"
# default thickness_ratio = 1
thickness_ratio = 2

# This flag controls if the topography is modified by the lobes and if the
# emplacement of new flows is affected by the changed slope
# topo_mod_flag = 0 => the slope does not change
# topo_mod_flag = 1 => the slope is re-evaluated every n_flows_counter flows
# topo_mod_flag = 2 => the slope is re-evaluated every n_lobes_counter flows
# and every n_flows_counter flows
topo_mod_flag = 1

# This parameter is only effective when topo_mod_flag = 1 and defines the
# number of flows for the re-evaluation of the slope modified by the flow
n_flows_counter = 1

# This parameter is only effective when topo_mod_flag = 2 and defines the
# number of lobes for the re-evaluation of the slope modified by the flow
n_lobes_counter = 500

# This parameter (between 0 and 1) allows for a thickening of the flow giving
# controlling the modification of the slope due to the presence of the flow.
# thickening_parameter = 0 => minimum thickening (maximum spreading)
# thickening_parameter = 1 => maximum thickening produced in the output
# default thickening_parameter = 0.2
# if you reduce this, the impact of the lava flow is lessened in the computation of the slope,
# but the thickness is still correct. this allows for "channel" flow, if = 1,
# then sublava flow would not happen.

```

thickening_parameter = 0.5

Lobe_exponent is associated to the probability that a new lobe will
be generated by a young or old (far or close to the vent when the
flag start_from_dist_flag=1) lobe. The closer is lobe_exponent to 0 the
larger is the probability that the new lobe will be generated from a
younger lobe.
lobe_exponent = 1 => there is a uniform probability distribution
assigned to all the existing lobes for the choice
of the next lobe from which a new lobe will be
generated.
lobe_exponent = 0 => the new lobe is generated from the last one.
This is very sensitive. As it goes up, the lava spreads out less and gets much thicker.
lobe_exponent = 0.18

max_slope_prob is related to the probability that the direction of
the new lobe is close to the maximum slope direction:
max_slope_prob = 0 => all the directions have the same probability;
max_slope_prob > 0 => the maximum slope direction has a larger
probability, and it increases with increasing
value of the parameter;
max_slope_prob = 1 => the direction of the new lobe is the maximum
slope direction.
default max_slope_prob = 0.8
This is very sensitive. If this is too low, then the randomness is driving the direction, and the
topography is not having a proper impact. keep greater than 0.5
max_slope_prob = 0.7

Inertial exponent:
inertial_exponent = 0 => the max probability direction for the new lobe is the
max slope direction;
inertial_exponent > 0 => the max probability direction for the new lobe takes
into account also the direction of the parent lobe and
the inertia increases with increasing exponent
default inertial_exponent = 0.125
inertial_exponent = 0.1

C. Grain size distribution from Heimaey 1973 eruption

During the 1973 eruption of Heimaey, a series of measurements of tephra deposits at defined sites were reported in Egilson (1974). Tephra was collected and sieved into different size bins and weighed. The time series of measurements made at eight sampling locations (Figure 4) were integrated to provide the total mass deposited over the duration of the eruption at each site and the percentage of tephra collected in each size bin, ranging from -4 – 5 phi (16–0.0313 mm). These tephra properties (Table 5) were used as input to the TOTGS (Total grain size distribution of tephra fallout) model (Biass & Bonadonna, 2014). This model uses Voronoi tessellation techniques on grain size distributions measured at sampling sites to calculate the total grain size distribution (TGSD) of tephra to be representative of the entire eruption (Bonadonna & Houghton, 2005). The total grain size distribution calculated this way is shown in Figure 11. This was used as the grain size distribution for the tephra simulations for the potential impact of future eruptions (Section 3.5).

Table 5: The cumulative mass and average size distribution of tephra samples reported in Egilson (1974).

Sampling site	Lat	Long	mass g/m ²	Phi wt%									
				-4	-3	-2	-1	0	1	2	3	4	5
9	63.438	-20.270	237	1.1	25.1	33.9	17.4	11.2	5.8	2.7	1.5	0.8	0.5
40 (G)	63.435	-20.268	325	0.3	7.4	21.5	21.9	23.9	16.5	5.6	1.8	0.7	0.5
30 (Hv)	63.439	-20.272	290	2.0	26.4	36.5	16.6	9.8	4.9	1.9	1.0	0.5	0.4
6 (Kó)	63.441	-20.269	269	0.4	6.2	16.0	22.4	27.0	18.8	6.4	1.7	0.6	0.4
36 (Mi)	63.442	-20.272	244	0.7	21.5	32.4	18.9	12.9	7.4	3.4	1.6	0.8	0.5
5 (Q)	63.437	-20.265	296	3.0	29.3	35.1	15.9	8.2	4.1	2.0	1.3	0.6	0.4
2 (Tm)	63.440	-20.276	288	1.5	24.3	32.5	14.8	11.8	8.7	3.8	1.6	0.7	0.4
56	63.437	-20.263	238	1.8	16.8	33.5	21.4	13.8	7.0	2.9	1.6	0.8	0.5

D. Age of vents relative to best fit line

To characterize alignment of mapped vents (Appendix A; Figure 2), a linear trend is fit to all 47 mapped locations (Figure 22).

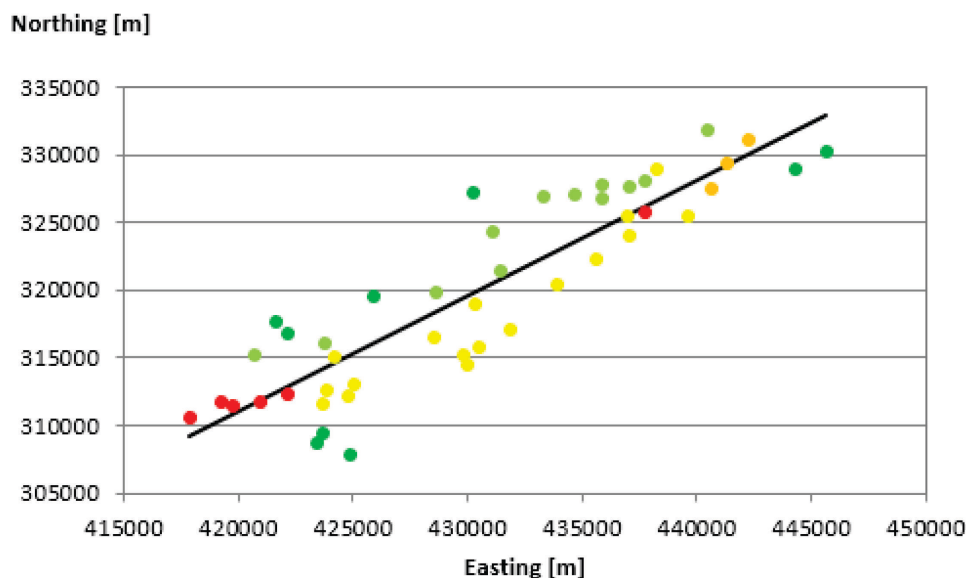


Figure 22: Spatial distribution of identified vents (dots) and the best fit line of their locations (black line). The dots are color coded as Historical: red; 2000–6000 BP: orange; 6000–10000 BP: yellow; 10000–13000 BP: light green; and 13000–16000: dark green. The calculation of the best fit line is independent of the vent ages.

The distances of the identified vents from the best fit line (Figure 22) are approximately normally distributed about the mean with a standard deviation of 2.5 km.

The relationship between the 47 identified vents to the best fit line was analyzed for each age bin (Figure 23). There is a correlation ($r_{\text{Spearman}} = 0.6$) showing that the older vents are generally found farther away from the central tendency line, while younger ones are generally closer to it (Figure 23). The tallest features of the region: islands and skerries above the sea surface, are found on or close to the orientation line, where older vents have been covered by eruptive products from younger eruptions. A single eruption, for example the Surtsey eruption, can leave evidence of multiple vents, or, for example the Eldfell eruption, can have had multiple events in the start of the eruption, but leave evidence of only one vent.

The Last Glacial Maximum ice sheet retreated from the area around 18,000–20,000 years BP (Höskuldsson et al., 2009). The pattern of vent ages and distance from the orientation line can be explained if, following the ice sheet retreat 16,000 years ago, eruption frequency decreased until the present time. In a time of higher eruption frequency, eruptions were distributed broadly, both proximal to and distal from the central tendency trend. As the eruption rate has reduced, so too has the potential for erupting further away from the alignment line. We interpret that future vents are most likely to open on the central line, and the likelihood of future vent openings decreases with distance.

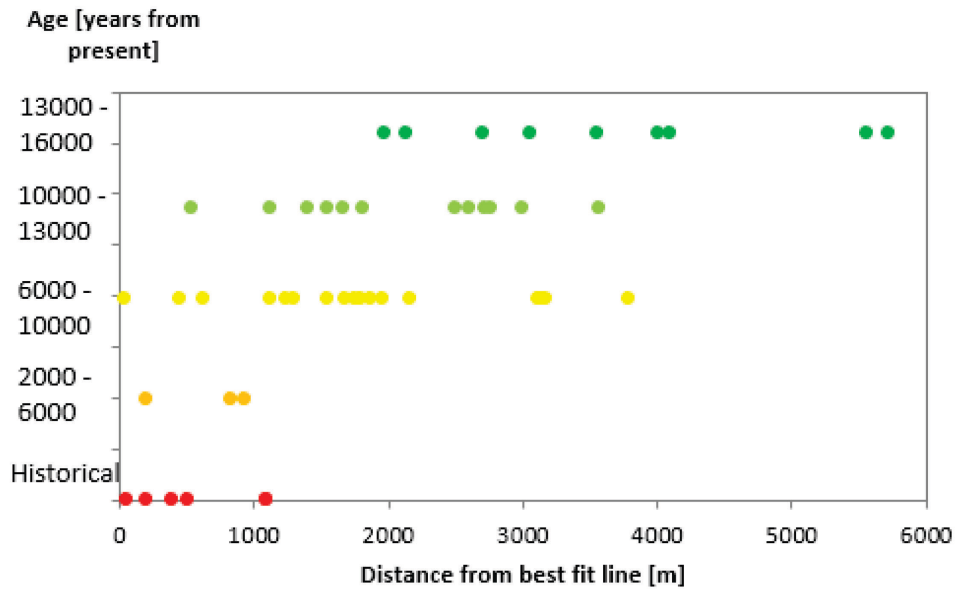


Figure 23: Distance from the best fit line of identified vents by age. The dots are color coded as: Historical, red; 2,000–6,000 BP, orange; 6,000–10,000 BP, yellow; 10,000–13,000 BP, light green; and 13,000–16,000, dark green.

E. Weight-bearing capacity of homes in Heimaey

The roofs of buildings in Iceland are classified according to presumed roof strength within a database maintained by the Real Estate Register of Registers Iceland. The suitability of this classification system for calculating susceptibility of roof collapse to mass loading was tested. The load bearing capacity for common residence roof types in Iceland: flat concrete slab, pitched timber roof on flat concrete slab, typical timber, timber truss, and timber other/unknown were calculated. Residences in Vestmannaeyjar were grouped by these roof types, and homes in each roof type were randomly chosen. Detailed calculations were made of individual roofs to determine their true load bearing capacity, and were compared with the load bearing capacity assumed for the roof strength category defined in the Real Estate Register (Table 6).

Table 6: Mass load capacity of Vestmannaeyjar residences by roof type.

Roof type	Number of residences	% of total	Load capacity [kg/m ²]			Presumed class strength ¹²	Load 50% will collapse [kg/m ²]
			min	mean	max		
Flat concrete slab	159	7	61	730	1794	Strong	714
Pitched timber roof on flat concrete slab	260	12	133	566	877	Medium strong	459
Typical timber	708	33	255	556	1437	Medium strong	459
Timber truss	111	5	296	807	1346	Strong	714
Timber other/unknown	664	31	194	561	1157	Medium strong	459
Uncategorized	234	11					
All roofs	2136	100	61	588	1794	Medium	459

The data were analyzed to determine if the four distinctive roof types (excluding roof type “Timber other/unknown”) were statistically unique from each other, i.e. if it is statistically sound to generalize the roof strength based on these roof type categories. We found that only timber truss roofs are unique from the other roof types: the three other categories could not be distinguished from each other. We used t-test result <0.1 to indicate uniqueness. T-test results for timber truss = 0.09 vs. flat concrete slab, 0.01 vs. pitched timber roof on flat concrete slab, and 0.00 vs. typical timber. Timber truss roofs have the strongest roofs on average, but individual roofs within the flat concrete slab and typical timber categories are stronger than the strongest individual roof within the timber truss category. We find that the roof types are not

¹² The proposed classification of European roof types using the categories of weak, medium weak, medium strong, and strong, and the associated mean collapse load are from Spence et al., 2005.

sufficiently unique to distinguish the load-bearing capacity by roof type, but rather it is appropriate to apply the average of the subset of roofs that were analyzed in detail to all the residences in Heimaey. This means that we calculate that 50% of the roofs of residences in Heimaey will collapse at 588 kg/m^2 , while 50% would be expected to withstand this mass loading. In contrast, if we used the presumed load bearing capacity of the “Medium strong” class (Spence et al., 2005), the average collapse would occur at 459 kg/m^2 . As a group, the residences in Heimaey can bear more load than the assumed values, however, there is a tremendous variance in the load bearing capacity of individual residences, and some roofs will collapse under much less load than the others. The impact of using 588 kg/m^2 as opposed to 459 kg/m^2 is shown in Figure 24. A simulation was made of the transport and deposition of tephra produced during the first week of the 1973 Eldfell eruption. This figure shows that an assumption of 50% residence roof collapse at 588 kg/m^2 as opposed to 459 kg/m^2 has a significantly different result for analyzing eruption impact.

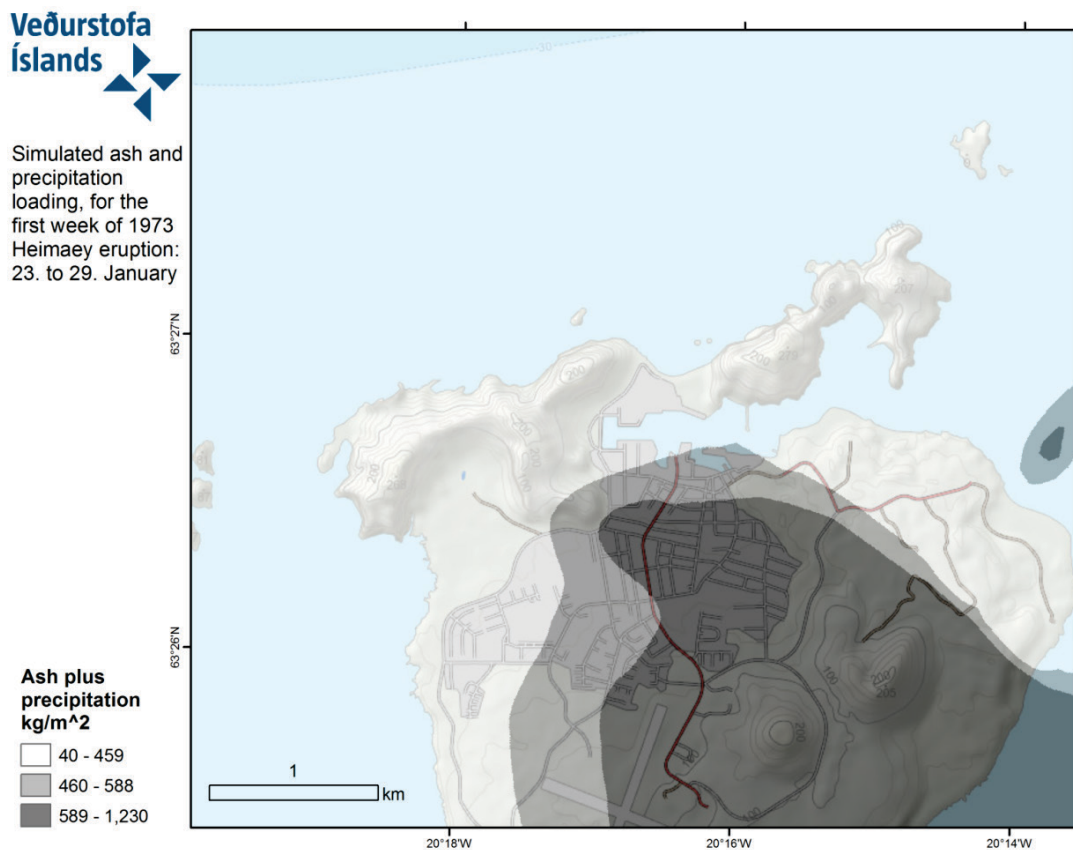


Figure 24: Simulated mass loading (tephra + precipitation) for 23–29 January 1973 during the Eldfell eruption.

F. How to contextualize the probabilities given in this report

The long-term eruption frequency of the Vestmannaeyjar volcanic system is poorly known. It is on the order of one cluster of eruptions/thousands of years. One eruption/1,000 years, as reported in (Höskuldsson, 2015), gives a yearly eruption probability of 0.001. This is **not a robust solution**, which is why it is not included in the main text. It is included here in the appendices so that we can provide some context for the probabilities provided in this report.

Consider the parts of Heimaey with greater than 1% (0.01) probability of being inundated with lava during the next eruption of the Vestmannaeyjar system that originates on Heimaey (Figure 8). If we multiply this 0.01 probability of being inundated by lava by the 0.001 probability of an eruption each year in the volcanic system, this means there is a 0.00001 probability of the most densely populated parts of Heimaey being inundated by lava each year if an eruption of the volcanic system occurs on Heimaey.

The acceptable annual probability of being killed in an avalanche in a home has been defined to be 0.00003 and, in a workplace, to be 0.0001. It is not necessarily correct to apply the same acceptable annual probability of being killed in an avalanche to be equivalent to the acceptable annual probability of an infrastructure being destroyed, via mass loading or being inundated by lava. The first is about deaths while the second is about economic harm, if we assume that people in a building would be evacuated prior to destruction of the building.

As we do not have a robust solution for the temporal eruption occurrence, and we do not have a defined acceptable risk for infrastructure destruction, we have analyzed the economic cost of infrastructure destruction using discretized steps of acceptable risk, with calculations made for risk thresholds of building destruction at 5% steps from 5% to 40%. These results are shown in Figure 21.

We provide here two complete tables for 5% (Table 7) and 25% (Table 8) thresholds, to show how the economic cost to different categories of infrastructure changes due to the different scenarios. When there is a zero in the table, it means that no infrastructure in that category met the given acceptable risk threshold. For example, the model of future vent opening based on the best fit line (Figure 16) reduces the likelihood of lava inundation in the developed areas to the point that no infrastructure is modeled to be at a greater than 25% likelihood of inundation given all lava flow (large, moderate, and small) scenarios. The 25% threshold is less likely to be reached than the 5% threshold, so the possible economic harm is reduced using a higher threshold (a higher threshold is less conservative).

Table 7: Potential economic impact in Heimaey using an acceptable risk threshold of 5% for tephra deposits and lava inundation based on structure values from November 2017 in thousands of ISK.

Description	IST120:2012	> 5%			Moderate lava flow			
		Saturated tephra	Large lava flow		Unweighted	Normal	Gaussian kernel	
		Thousands of ISK						
		Unweighted	Normal	Gaussian kernel	Unweighted	Normal	Gaussian kernel	
Residential buildings	1000;1100; 1200	70,907,781	69,910,705	65,909,605	68,162,645	69,823,851	56,819,175	63,611,225
Hotels and other specialized residential structures	1300	Not included	774,450	774,450	774,450	774,450	774,450	774,450
Commercial buildings	2000	Not included	23,576,580	23,576,580	23,576,580	23,576,580	23,576,580	23,576,580
Industrial buildings	2600	Not included	323,650	323,650	323,650	323,650	323,650	323,650
Public assembly structures	3000; 3200; 3500; 3800	Not included	5,232,050	5,232,050	5,232,050	5,232,050	5,232,050	5,232,050
Airport facilities	3920; 5600	Not included	817,700	0	0	876,750	0	0
Institutional or community facilities	4000; 4200; 4400; 4500	Not included	5,900,400	5,900,400	5,900,400	5,900,400	4,942,150	5,900,400
Medical facilities	4100	Not included	1,608,350	1,608,350	1,608,350	1,608,350	1,608,350	1,608,350
Utility structures	6200; 6300; 6400	Not included	528,500	528,500	528,500	528,500	353,900	353,900
Total (thousands of ISK)		70,907,781	108,672,385	103,853,585	106,106,625	108,644,581	93,630,305	101,380,605
% of total value of structures on Heimaey		64	98	94	96	98	84	91

Description of IST120:2012 codes: 1000: Residential buildings; 1100: Single family buildings; 1200: Multifamily structures; 1300: Other specialized residential structures; 2000: Commercial buildings and other specialized structures; 2600: Industrial buildings and structures; 3000: Public assembly structures; 3200: Indoor games facility; 3500: Churches, synagogues, temples, mosques, etc.; 3800: Other community structures; 3920: Airport terminal; 5600: Air and space transportation facility; 4000: Institutional or community facilities; 4200: School or university buildings; 4400: Museum, exhibition, or similar facility; 4500: Public safety-related facility; 4100: Medical facility; 6200: Water-supply-related facility; 6300: Sewer and waste-related facility; 6400: Gas or electric power generation facility.

Table 8: Potential economic impact in Heimaey using an acceptable risk threshold of 25% for tephra deposits and lava inundation based on structure values from November 2017 in thousands of ISK.

> 25%	Saturated tephra	Large lava flow			Moderate lava flow			
		Thousands of ISK						
Description	IST120:2012		Unweighted	Normal	Gaussian kernel	Unweighted	Normal	Gaussian kernel
Residential buildings	1000;1100; 1200	4,220,937	55,477,035	0	2,058,360	32,529,065	0	0
Hotels and other specialized residential structures	1300	Not included	774,450	0	120,050	271,150	0	0
Commercial buildings	2000	Not included	23,576,580	0	9,153,980	18,513,690	0	0
Industrial buildings	2600	Not included	323,650	0	226,400	323,650	0	0
Public assembly structures	3000; 3200; 3500; 3800	Not included	5,232,050	0	117,800	4,938,000	0	0
Airport facilities	3920; 5600	Not included	0	0	0	0	0	0
Institutional or community facilities	4000; 4200; 4400; 4500	Not included	4,942,150	0	13,750	3,025,850	0	0
Medical facilities	4100	Not included	1,608,350	0	0	1,608,350	0	0
Utility structures	6200; 6300; 6400	Not included	353,900	0	0	5,050	0	0
Total (thousands of ISK)		4,220,937	92,288,165	0	11,690,340	61,214,805	0	0
% of total value of structures on Heimaey		4	83	0	11	55	0	0

Description of IST120:2012 codes: 1000: Residential buildings; 1100: Single family buildings; 1200: Multifamily structures; 1300: Other specialized residential structures; 2000: Commercial buildings and other specialized structures; 2600: Industrial buildings and structures; 3000: Public assembly structures; 3200: Indoor games facility; 3500: Churches, synagogues, temples, mosques, etc.; 3800: Other community structures; 3920: Airport terminal; 5600: Air and space transportation facility; 4000: Institutional or community facilities; 4200: School or university buildings; 4400: Museum, exhibition, or similar facility; 4500: Public safety-related facility; 4100: Medical facility; 6200: Water-supply-related facility; 6300: Sewer and waste-related facility; 6400: Gas or electric power generation facility.
